



# NAVAL POSTGRADUATE SCHOOL

## Monterey, California

AD-A275 003



DTIC  
ELECTE  
JAN 27 1994  
S E D

## THESIS

FLOW VISUALIZATION AND EXPERIMENTAL  
OPTIMIZATION OF THREE INLET-SIDE-DUMP  
LIQUID-FUEL RAMJET COMBUSTORS

by

Ronald Frank Salyer

September, 1993

Thesis Advisor:

Prof D.W. Netzer

Approved for public release; distribution is unlimited.

94-02777



94 1 26 203

# REPORT DOCUMENTATION PAGE

Form Approved OMB No. 0704

Public reporting burden for this collection of information is estimated to average 1 hour per response, including the time for reviewing instruction, searching existing data sources, gathering and maintaining the data needed, and completing and reviewing the collection of information. Send comments regarding this burden estimate or any other aspect of this collection of information, including suggestions for reducing this burden, to Washington Headquarters Services, Directorate for Information Operations and Reports, 1215 Jefferson Davis Highway, Suite 1204, Arlington, VA 22202-4302, and to the Office of Management and Budget, Paperwork Reduction Project (0704-0188) Washington DC 20503.

1. AGENCY USE ONLY ( <i>Leave blank</i> )	2. REPORT DATE 1993, September.	3. REPORT TYPE AND DATES COVERED Master's Thesis	
4. TITLE AND SUBTITLE FLOW-VISUALIZATION AND EXPERIMENTAL OPTIMIZATION OF THREE INLET-SIDE-DUMP LIQUID-FUEL RAMJET COMBUSTORS		5. FUNDING NUMBERS	
6. AUTHOR(S) Ronald F. Salyer			
7. PERFORMING ORGANIZATION NAME(S) AND ADDRESS(ES) Naval Postgraduate School Monterey CA 93943-5000		8. PERFORMING ORGANIZATION REPORT NUMBER	
9. SPONSORING/MONITORING AGENCY NAME(S) AND ADDRESS(ES) Naval Air Warfare Center, Weapons Division China Lake, CA 93555		10. SPONSORING/MONITORING AGENCY REPORT NUMBER	
11. SUPPLEMENTARY NOTES The views expressed in this thesis are those of the author and do not reflect the official policy or position of the Department of Defense or the U.S. Government.			
12a. DISTRIBUTION/AVAILABILITY STATEMENT Approved for public release; distribution is unlimited.		12b. DISTRIBUTION CODE *A	
13. ABSTRACT ( <i>maximum 200 words</i> ) Three distinct inlet-side-dump ramjet-combustor geometric configurations were investigated. Non-intrusive water-tunnel flow-visualization techniques were utilized to qualitatively determine optimum flame-stabilization dome lengths and fuel-injection locations. The results were in good agreement with the results from previous studies. The optimum dome lengths which provided good fuel distribution and steady mixing all had lengths between 0.31 D and 1.4 D. Fuel injection in a narrow region on the upstream side of the inlet cross section was the only location capable of distributing fuel into the flame-holding region. Multiple injection locations in the inlet were required to distribute fuel uniformly into the main combustion region. The dual, axially-in-line side-dump configuration demonstrated the best potential for increasing performance across a wide range of operating conditions due to the ancillary combustion region between the inlets and the ability to control the size and strength of the region by varying air mass flow through the two inlet dumps.			
14. SUBJECT TERMS Side Dump Combustor Ramjet Flow-Visualization		15. NUMBER OF PAGES 75	
		16. PRICE CODE	
17. SECURITY CLASSIFICATION OF REPORT Unclassified	18. SECURITY CLASSIFICATION OF THIS PAGE Unclassified	19. SECURITY CLASSIFICATION OF ABSTRACT Unclassified	20. LIMITATION OF ABSTRACT UL

NSN 7540-01-280-5500

Standard Form 298 (Rev. 2-89)

Prescribed by ANSI Std. Z39-18

Approved for public release; distribution is unlimited.

Flow Visualization and Experimental Optimization of  
Three Inlet-Side-Dump Liquid-Fuel  
Ramjet Combustors

by

Ronald F. Salyer  
Major, United States Army  
B.S., United States Military Academy, 1981

Submitted in partial fulfillment  
of the requirements for the degree of

MASTER OF SCIENCE IN AERONAUTICAL ENGINEERING

from the

NAVAL POSTGRADUATE SCHOOL

September 1993

Author:

Ronald J. Salyer

Approved by:

Ronald F. Salyer

David W. Netzer

David W. Netzer, Thesis Advisor

Raymond P. Shreeve

Raymond P. Shreeve, Second Reader

Daniel J. Collins

Daniel J. Collins, Chairman

Department of Aeronautics and Astronautics

## ABSTRACT

Three distinct inlet-side-dump ramjet-combustor geometric configurations were investigated. Non-intrusive water-tunnel flow-visualization techniques were utilized to qualitatively determine optimum flame-stabilization dome lengths and fuel-injection locations. The results were in good agreement with the results from previous studies. The optimum dome lengths which provided good fuel distribution and steady mixing all had lengths between 0.31 D and 1.4 D. Fuel injection in a narrow region on the upstream side of the inlet cross section was the only location capable of distributing fuel into the flame-holding region. Multiple injection locations in the inlet were required to distribute fuel uniformly into the main combustion region. The dual, axially-in-line side-dump configuration demonstrated the best potential for increasing performance across a wide range of operating conditions due to the ancillary combustion region between the inlets and the ability to control the size and strength of the region by varying air mass flow through the two inlet dumps.

Accession For	
NTIS	CRA&I
DTIC	TAB
Unannounced	
Justification _____	
By _____	
Distribution / _____	
Availability Codes	
Dist	Avail and / or Special
A-1	

DTIC QUALITY INSPECTED 5

## TABLE OF CONTENTS

I.	INTRODUCTION .....	1
II.	EXPERIMENTAL APPARATUS AND PROCEDURES .....	10
	A. Combustor Flow-Visualization Apparatus.....	10
	B. Flow-Visualization Experimental Procedures.....	17
III.	RESULTS .....	24
	A. Single-Side-Dump Combustor.....	25
	B. Dual-Inlet Side-Dump Combustor with Inlets Separated by 90°.....	39
	C. Dual, In-line Side-Dump Combustor.....	48
	D. Comparison of the Results with Other Investigations.....	60
IV.	CONCLUSIONS.....	62
	LIST OF REFERENCES .....	64
	INITIAL DISTRIBUTION LIST .....	66

## LIST OF FIGURES

1.1	Typical Integral-Rocket-Ramjet Configuration.....	2
2.1	Schematic of Flow-Visualization Test Facility.....	11
2.2	Schematic of Flow-Visualization Experimental Setup.....	13
2.3	Photograph of Water-Tunnel Experimental Setup.....	13
2.4	Experimental Combustor-Model Geometries.....	14
2.5	Plexiglas Combustor-Model Configurations.....	15
2.6	"Fuel" Manifold and "Fuel" Injection Schemes.....	17
2.7	Reference Coordinate System.....	19
3.1	Configuration 1 in Operation in the Water Tunnel.....	26
3.2	Configuration 1; Dome Region, $L_d=-1"$ , $L_{1z}=0"$ .....	28
3.3	Configuration 1; Dome Region, $L_d=-1"$ , $L_{1x}=1"$ .....	28
3.4	Configuration 1; Dome Region, $L_d=-1"$ , $L_{1z}=1"$ .....	29
3.5	Configuration 1; Dome Region, $L_d=-1"$ , $L_{1z}=1.5"$ .....	29
3.6	Configuration 1; Dome Region, $L_d=-4"$ , $L_{1y}=.5"$ .....	30
3.7	Configuration 1; Dome Region, $L_d=0"$ , $L_{1y}=1"$ .....	30
3.8	Configuration 1; Dome Region, $L_d=-4"$ , $L_{1z}=0"$ .....	31
3.9	Configuration 1; Main Combustor, $L_d=-4"$ , $L_{1y}=3.5"$ .....	33
3.10	Configuration 1; Longitudinal Circulation Center ( $L_c$ ) Versus Dome Length ( $L_d$ ).....	35
3.11	Impact of "Fuel" Injection Location on "Fuel" Distribution, Configuration 1.....	38

3.12 Configuration 2; Top View, Dome Region, $L_d=0"$ , $L_{1x}=1"$ .....	41
3.13 Configuration 2; Dome Region, $L_d=-4"$ , $L_{1z}=0"$ .....	41
3.14 Configuration 2; Bottom View, Dome Region, $L_d=0"$ , $L_{1z}=0"$ .....	42
3.15 Configuration 2; Dome Region, $L_d=0"$ , $L_{1z}=0"$ .....	42
3.16 Configuration 2; Longitudinal Circulation Center ( $L_c$ ) Versus Dome Length ( $L_d$ ).....	44
3.17 Impact of "Fuel" Injection Location on "Fuel" Distribution, Configuration 2.....	47
3.18 Configuration 3: Dual-Inlet, Axially-In-Line, Side- Dump Combustor.....	49
3.19 Configuration 3; Dome Region, $L_d=-3"$ , $L_{1x}=0$ .....	50
3.20 Configuration 3; Region 2, $L_d=-3"$ , $L_{1x}=0$ .....	51
3.21 Configuration 3; Region 2, $m_1/m_2=85/15\%$ , $L_d=-2"$ , $L_{1x}=1.5"$ .....	52
3.22 Configuration 3; Dome Region, $L_d=-2"$ .....	53
3.23 Configuration 3; $L_d=4.5"$ .....	53
3.24 Configuration 3; Region 2, $m_1/m_2=85/15\%$ , $L_d=-4"$ , $L_{1x}=0"$ .....	54
3.25 Configuration 3; Longitudinal Circulation Center ( $L_c$ ) Versus Dome Length ( $L_d$ ).....	56
3.26 Configuration 3; Region 2, $m_1/m_2=50/50\%$ , $L_d=-2"$ , $L_{1x}=0"$ .....	58

3.27 Configuration 3; Region 2, $m_1/m_2=50/50\%$ , $L_d=-2"$ ,	
$L_{lx}=0"$ .....	58
3.28 Impact of "Fuel" Injection Location on "Fuel" Distribution, Configuration 3.....	59

**LIST OF TABLES**

<b>3.1 SUMMARY AND COMPARISON OF RESULTS FOR SIDE-DUMP COMBUSTORS.....</b>	<b>61</b>
--	-----------

## I. INTRODUCTION

Modern propulsion systems such as the turbojet, turbofan, rocket engine and ramjet offer designers and engineers numerous performance trade-offs in order to obtain the optimum capability for specific mission profiles. Relatively low-cost ramjet engines are increasingly popular because of their suitability for tactical-missile applications, especially with the increased emphasis on stand-off surgical strikes that do not endanger friendly aircraft or personnel. Generally, ramjet engines offer the best cycle efficiency over a wide range of supersonic Mach numbers and flight conditions of all air-breathing propulsion systems [Ref. 1]. Of particular interest are designs that combine the benefits of solid rocket and ramjet technology since they are ideally suited for volume-limited tactical-missile applications. Integral-Rocket Ramjets (IRR) offer increased versatility due to the rapid acceleration provided by a simple, low-weight, solid-rocket booster integrated with the compactness and increased range of a side-dump inlet liquid-fuel ramjet. IRR configurations as shown in Figure 1.1 include a combustion chamber initially filled with solid propellant for the boost phase of flight. The booster accelerates the system to  $M_\infty \sim 2-2.5$ , after

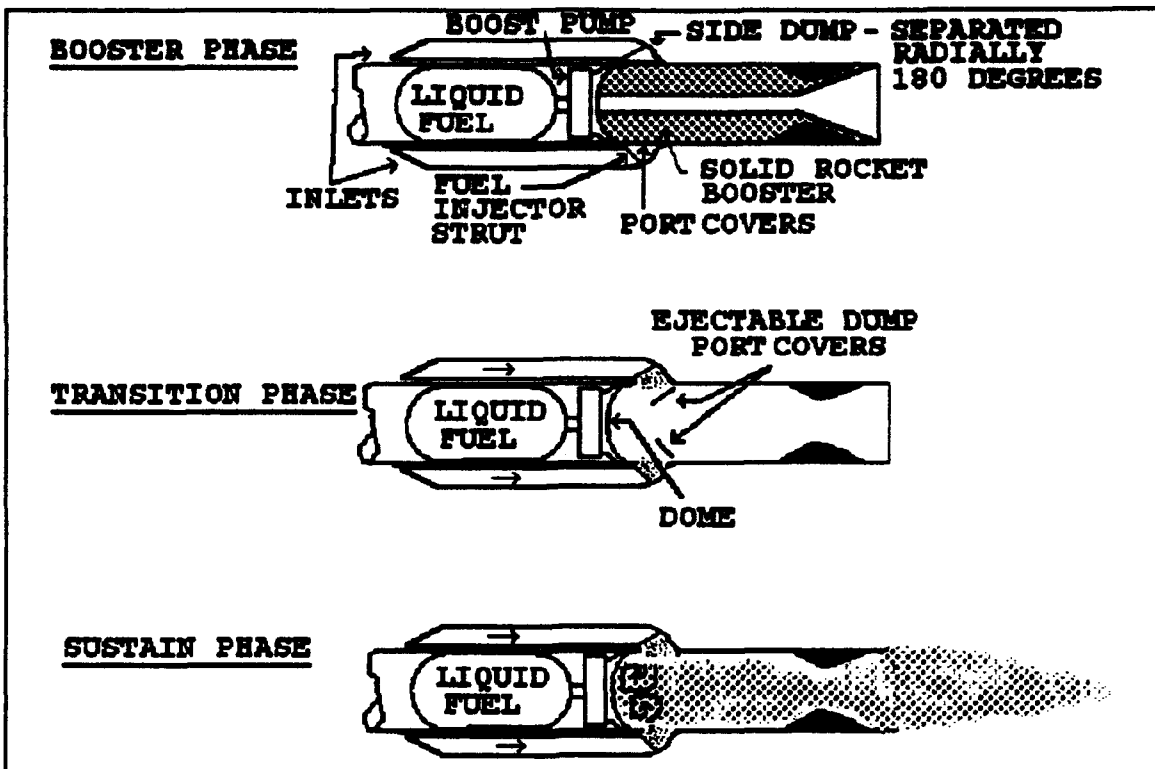


**Figure 1.1:** Typical Integral-Rocket-Ramjet Configuration [adapted from Ref. 2]

which the ramjet sustain mode is maintained for the balance of the flight time. Once the solid rocket propellant is expended, side-dump inlet-port covers are ejected to allow air injection into the combustion chamber from the missile inlets. Liquid fuel is injected into the air flow inside the side dumps and flame stability is accomplished in the combustion chamber by aerodynamic flame holding in mixing and recirculation zones. The reliance on aerodynamic flame holding is necessitated by the solid propellant booster, which prohibits the use of injectors or bluff-body flame holders directly in the combustion chamber. It is highly desirable, therefore, to optimize ramjet combustor design to take

advantage of the combustor aerodynamics and combustion dynamics in order to provide the highest possible performance over the widest possible range of flight conditions.

Optimizing ramjet combustor performance consists primarily of ensuring flame stability, efficient combustion, and minimizing total pressure losses, while remaining within volume/size limitations imposed by mission or application constraints.

Efficient combustion at typical ramjet pressures (10-200 psi) requires rapid vaporization of fuel and fuel-air mixing followed by rapid chemical reaction rates. For a given liquid fuel, the chemical reaction rates are a function of the combustion chamber static pressure, the inlet air temperature and the degree of mixing. Performance generally improves as the temperature and static pressure increase. Flame stability is also important and is directly affected by flow velocity. High flow velocity in the flame region may blow out the flame while low velocity may allow the flame to migrate to the fuel injection source and be extinguished. Thus, recirculation zones should provide areas of low local velocity to keep the flame stationary and ensure uniform burning as well as simultaneously providing increased turbulence to enhance mixing and energy transfer from the zone. Also, flammability depends upon the equivalence ratio. A very lean or very rich fuel-air ratio can reduce temperatures below the point at which the vaporized fuel and inlet air can react. Thus, it is

desirable to have high pressure (reaction rates) and large combustor volume with relatively low mass flow rates together with good mixing and a suitable equivalence ratio. Typical ramjet operating envelopes require very wide ranges in equivalence ratios and air mass flow rates. These conditions make it difficult to maintain flammability and high combustion efficiency over the entire envelope.

Combustor total pressure loss is caused by diffuser/inlet turn and dump losses as well as combustor "cold flow" and heat addition losses. The turning of inlet air and rapid expansion of the air into the combustor volume causes undesirable stagnation pressure losses. This loss is primarily a function of dump angle, inlet Mach number and expansion ratio. "Cold flow" losses result from both friction and drag. "Cold Flow" losses increase as flow Mach number increases. Heat addition losses are primarily the result of increasing the entropy of the system, i.e. there is less energy available from combustion.

Another area of concern in side-dump ramjet combustors is combustion instability. Side-dump combustors can exhibit excessive levels of combustion instabilities in comparison to conventional axial-dump ramjet combustors. Oscillatory combustion often occurs when energy release processes within the combustor are able to amplify pressure and velocity disturbances and the combustor/inlet geometry and shock pattern are able to respond to further aggravate the

disturbances. These oscillations can lead to unchoking of the inlet diffuser (inlet "buzz"), flame-out, or catastrophic combustor case or nozzle structural failure. Decreasing the coupling of input energy with cavity resonance and increasing oscillation damping (energy loss mechanisms) are the most common methods of preventing and eliminating combustor oscillations. Analytical prediction of combustion oscillation remains inadequate since practical non-linear theory is in its developmental infancy. Thus, empirical evaluation of specific combustor geometries is essential to achieve optimal design and performance.

The combustor flow pattern that results from the side dump(s) is characterized by three-dimensional, turbulent mixing, swirling, impinging, reactive fluid dynamics. Hence, the complex nature of side-dump combustor fluid dynamics and combustion processes are not yet fully characterized and predictable. Computational methods for combustors in conventional turbojets and turbofan engines have been successfully modelled, yet empirical testing of designs remain essential [Ref. 3]. These computational methods have had more limited application to the ramjet combustor [Ref. 4,5]. Also, the models have not been adequately validated. Empirical methods, however, have continued to provide for adequate development of side-dump combustors. Traditionally, "cold-flow" visualization of a proposed combustor design precedes reacting-flow testing to provide

some understanding of the flow dynamics and possible instability sources. Qualitative mixing analysis and semi-quantitative analysis (with LDV) of the flow complexities are often conducted, although combustion effects cannot be fully represented. Follow-on, reacting-flow testing is typically used to validate "cold-flow" analysis by providing measurement of mechanisms that may induce combustion instabilities, and by analyzing the effects of fuel-air ratio on combustion efficiency.

Generally, it is desired to have a combustion chamber with a large volume available for complete combustion of fuel and oxidizer. The large volume ensures long residence times and thus complete burning of fuel and oxidizer. Large combustor volumes are normally not available in tactical-missile applications due to carrying constraints as well as other practical mission constraints. Thus, it is essential to optimize available combustor volume to ensure the best possible combustion efficiency over the mission envelope. Additionally, it is impractical for tactical-missile applications to have a dome-recirculation region greater than approximately two combustor diameters in length.

Numerous studies have contributed to the understanding of the complex flow and combustion processes of the side-dump ramjet combustor. Many of these studies have evaluated the impact of combustor geometry on combustor aerodynamics and combustor performance. Most of these studies used "cold-flow"

visualization to aid in designing and testing the performance of an actual ramjet combustor. The majority of these studies examined single side-dump or circumferentially-symmetric dual side-dump combustors. Petkus and Jaul [Ref. 6], in a "cold-flow" study, showed that two distinct recirculation regions existed for a single side-dump combustor when air and fuel were injected at  $90^\circ$  to the combustor longitudinal axis. One region (the flame-stabilization region) was forward of the dump plane, and was characterized by high mixing and relatively low local, yet steady, velocities depending on dome length. The second region was downstream of the dump plane and was characterized by slow, unsteady, recirculating flow which was insensitive to dome length and provided extended residence time in the combustor. In a similar study, Liou and Wu [Ref. 7] showed that the second recirculation zone did not exist for side-dump angles less than  $75^\circ$ . The flow became dominated by swirling vortices downstream of the inlet side dump. Stull et. al. [Ref. 8] used flow visualization and a LDV coupled with CFD code analysis to optimize the design of a dual,  $90^\circ$ -separated, rectangular-inlet side-dump, liquid-fuel ramjet combustor with variable side-dump angles. They measured the effects of varying dome length, dump angle and dump-entry air temperature on combustion efficiency of the ramjet combustor. They found that performance was insensitive to dome length and that performance was only slightly affected by inlet dump angle. The best performance was provided by a

45° inlet dump angle for high fuel-air ratios, and only marginally better performance was provided by a 60° inlet dump angle for low fuel-air ratios. Combustion efficiency was significantly affected by inlet air temperature, particularly at low fuel-air ratios. Efficiencies increased as inlet temperature increased, but reached a maximum level for fuel-air ratios greater than 0.05. Choudhury [Ref. 9] investigated the effects of introducing swirling flow into the side dump combustor compared to non-swirling cases and found that the size and strength of the recirculation zone in the dome region was a strong function of dome length and the pattern was crucial to combustor stability. Zetterström and Sjöblom [Ref. 10] studied the performance of two- and four-inlet side-dump combustors. The results from the two-side-dump combustor were of particular interest since four side dumps are often considered excessive and complex for volume-limited ramjet combustors in tactical-missile applications. The dual-inlet, 150° circumferentially-separated, 30° side-dump-angle combustor exhibited flow instabilities attributed to pressure oscillations caused by vortex shedding in the combustion chamber, which resulted in decreased combustor performance. The flow instabilities and pressure oscillations were successfully reduced by asymmetric fuel injection and by increasing inlet-air temperatures, which improved performance to acceptable levels. Clark [Ref. 11], investigating pressure oscillations that resulted in combustor test failures,

suggested the use of air-turning vanes in the inlet side dump to reduce the oscillations and prevent coupling with inlet and diffuser dynamics.

The main objective of the present study was to use water-tunnel flow-visualization techniques to characterize and compare the flow field in three combustors with variant geometric configurations that are currently under consideration at the Naval Air Warfare Center Weapons Division, China Lake, CA. The ultimate goal of this study was to provide data to optimize the flow conditions in order to increase performance over a wide range of operating equivalence ratios and air mass-flow rates. To this end, a single, circular, side-dump baseline configuration, a dual, circular, inlet side-dump configuration with dumps circumferentially separated by 90°, and a dual, axially-in-line circular inlet-side-dump configuration were investigated. The results were compared to published results of similar studies. The in-line, side-dump configuration was of interest since little was known about the flow field or combustion characteristics of this configuration. Also, this configuration offers potential for employment in advanced tactical missiles equipped with ramjet engines. It was believed, that by varying the percentage of mass flow rate through each side dump, increased efficiencies and reduced losses could be obtained to provide increased performance over wider operating envelopes.

## **II. EXPERIMENTAL APPARATUS AND PROCEDURES**

### **A. COMBUSTOR FLOW-VISUALIZATION APPARATUS**

#### **1. Flow-Visualization Test Facility**

The Naval Postgraduate School Eidetic International, Flow-Visualization Water Tunnel, as shown schematically in Figure 2.1, was modified to accommodate closed-circuit flow visualization of Plexiglas combustor models. The modification entailed pumping water from the tunnel plenum section through PVC piping, separate from the existing system piping, into the combustor model mounted in the tunnel test section. The flow was then exhausted into the tunnel discharge plenum. Water flow external to the combustor model in the tunnel test section was not used except to provide index of refraction matching for the cylindrical Plexiglas model. This prevented the model from acting as a lens, distorting the visible images from inside the model. A one horsepower Pearless Model 620A, 160 gpm centrifugal pump was used to achieve a water flow Reynolds number greater than  $1 \times 10^5$  at the combustor exit, which is typical of actual combustors. A pitot-static type flow meter, with the capability of measuring flow from 20-160 gpm with  $\pm 10\%$  accuracy, was placed upstream of the combustor model inlet to monitor flow rate. The water-tunnel air/dye injection system was connected to the model fuel injection

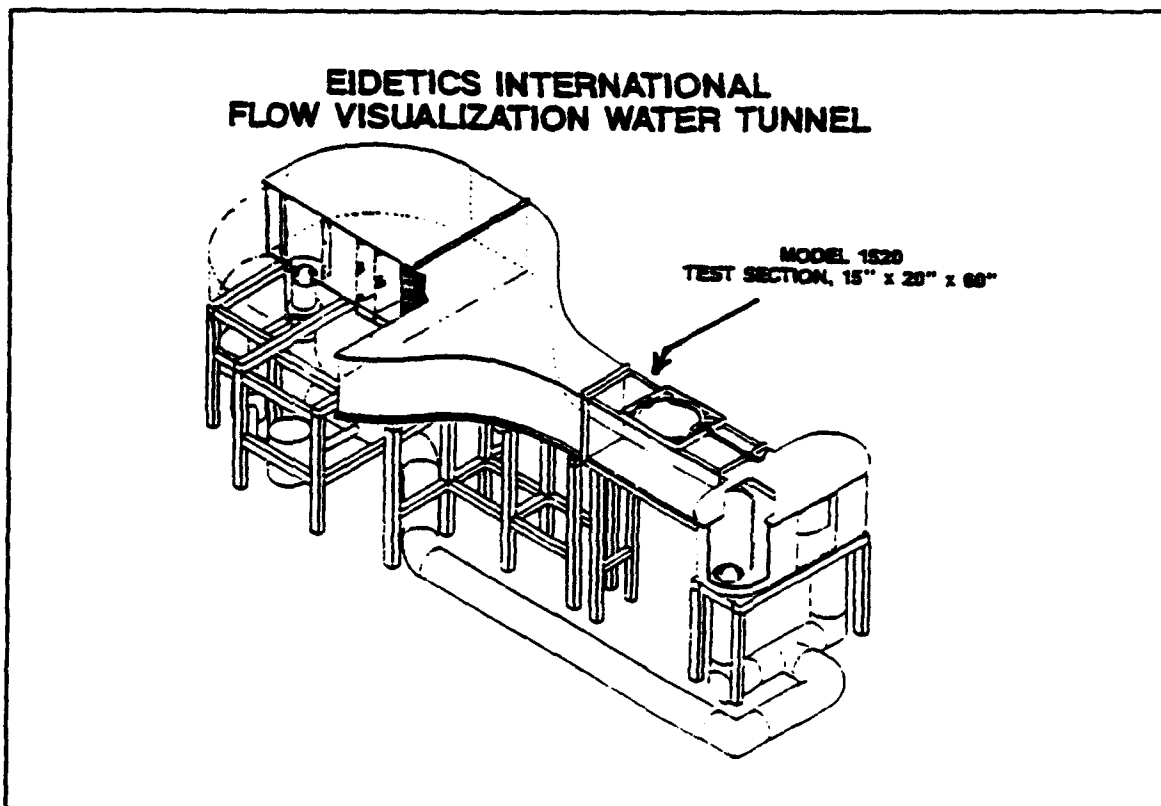


Figure 2.1: Schematic of Flow-Visualization Test Facility [Ref. 12]

manifold(s). It was used to inject small air bubbles or colored and fluorescent dyes for visualizing flow streamlines and "fuel" distribution patterns.

A 15 milliwatt helium-neon laser was used, in conjunction with a mirror and a 0.24 X 0.98 inch cylindrical lens, to provide a laser sheet through the test section and Plexiglas model. The laser sheet provided the capability to visualize two-dimensional flow conditions using time-elapsed photography of the scattered light from the tracer particles (air bubbles). The cylindrical lens provided a laser sheet approximately 0.08 inches thick at the center of the combustor

model. The sheet expanded to a width of approximately 5.0 inches at the center of the model. The laser and lens combination was repositioned during testing so that the width of the laser sheet was parallel to the flow in both the longitudinal and lateral planes. Additionally, the laser and lens combination was positioned so that the laser sheet was normal to the flow, providing a cross-sectional perspective of the flow. Small amounts of data were collected from this latter orientation due to visibility limitations imposed by the physical characteristics of both the model and the water tunnel.

Flow tests were documented by using a 55mm Single Lens Reflex (SLR) camera and a high resolution video camera. The 55mm SLR camera was manually operated, but was self-advancing, making rapid sequence photography possible. The camera had the standard range of shutter speeds and aperture settings. The video camera was capable of shutter speeds from 1/64 to 1/1000 seconds at multiple focal lengths. Both cameras were positioned at the side of, below, and above the combustor models to obtain data on the two dimensional longitudinal flow field from those perspectives. The cameras were also positioned to photograph, from an oblique angle, the flow field of the combustor cross section. Figure 2.2 and Figure 2.3 show a schematic and a photograph of the experimental setup respectively.

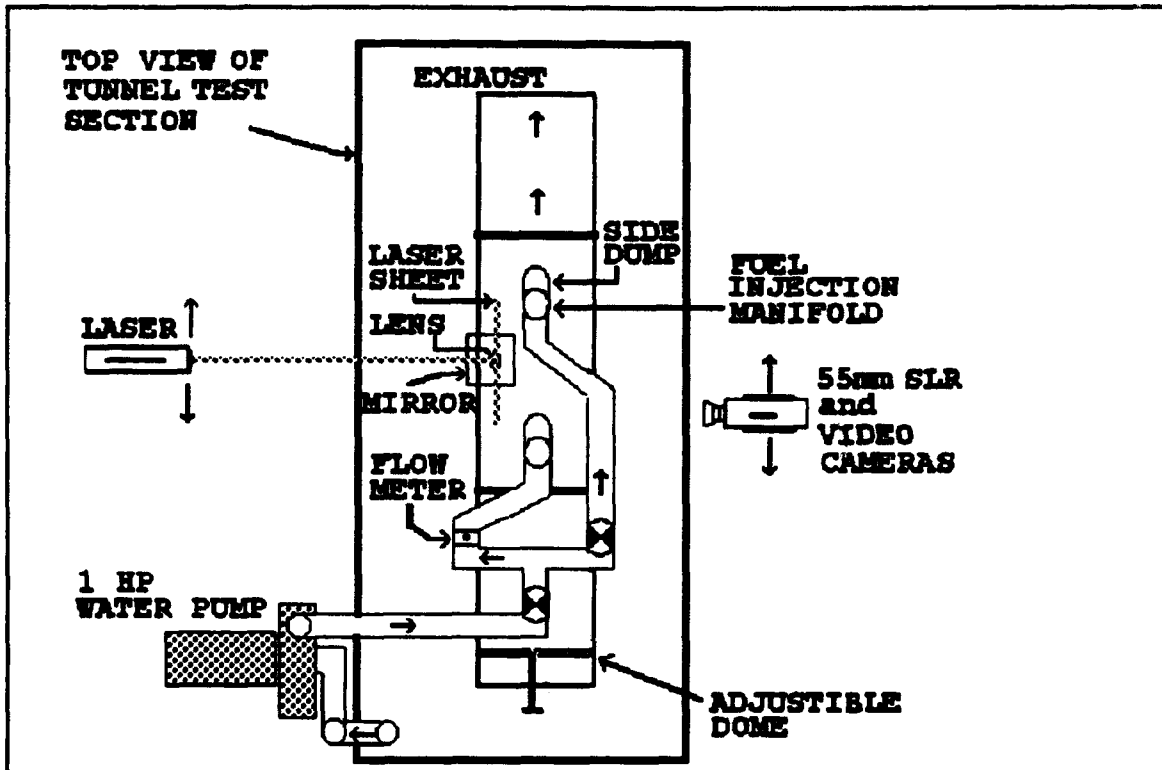


**Figure 2.2:** Schematic of Flow-Visualization Experimental Setup



**Figure 2.3:** Photograph of Water-Tunnel Experimental Setup

## 2. Flow-Visualization Combustor-Model Configurations

Three 0.125 inch thick Plexiglas combustor-model configurations were designed and fabricated for use in the flow-visualization facility. The geometries and physical dimensions are shown in Figure 2.4. Figure 2.5 is a photograph of the model configurations. All configurations utilized a 45° inlet-side-dump angle to minimize turn and dump losses. The combustor inner diameter was 3.25 inches, which corresponded to the dimensions of an existing sub-scale ramjet

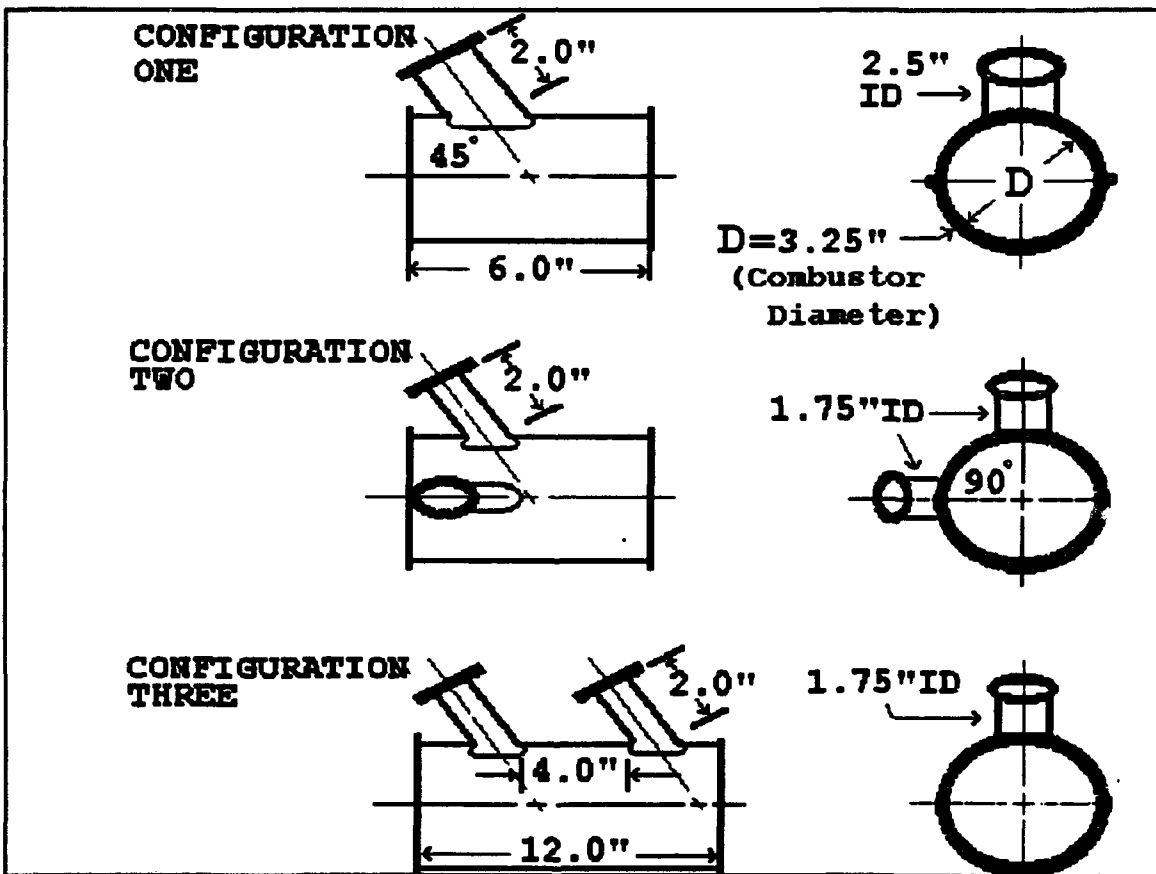


Figure 2.4: Experimental Combustor-Model Geometries

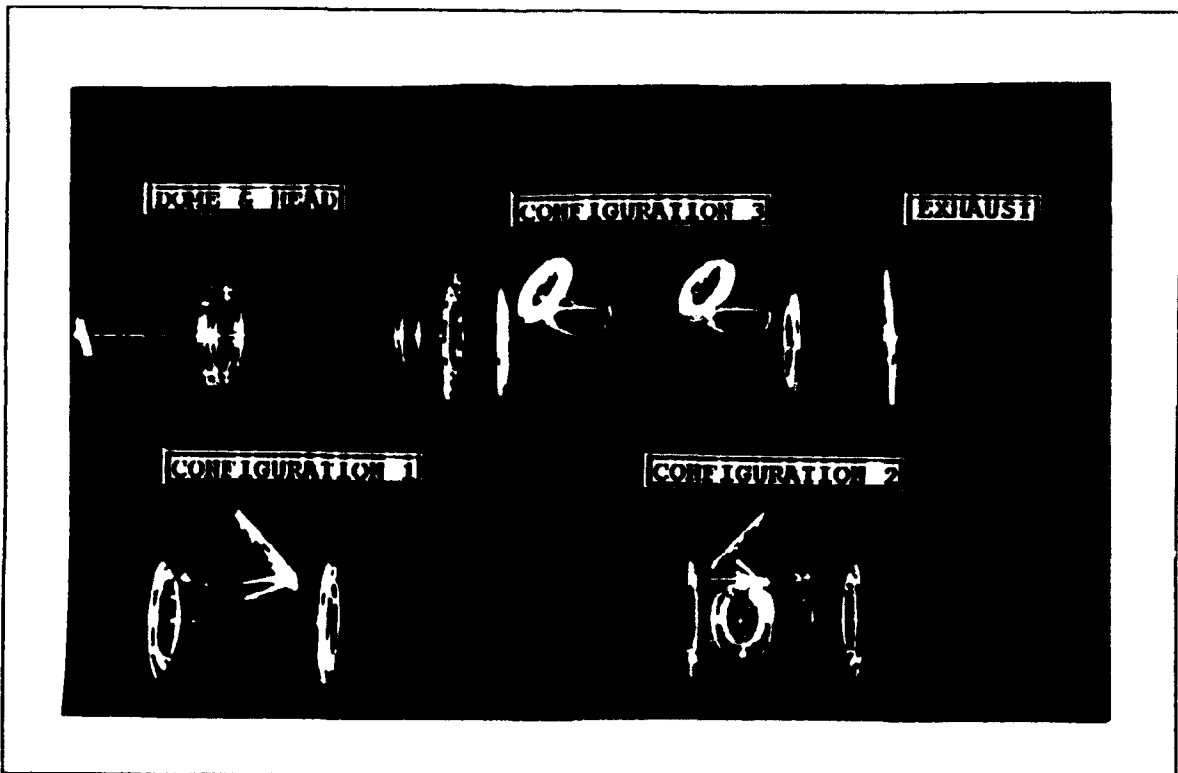
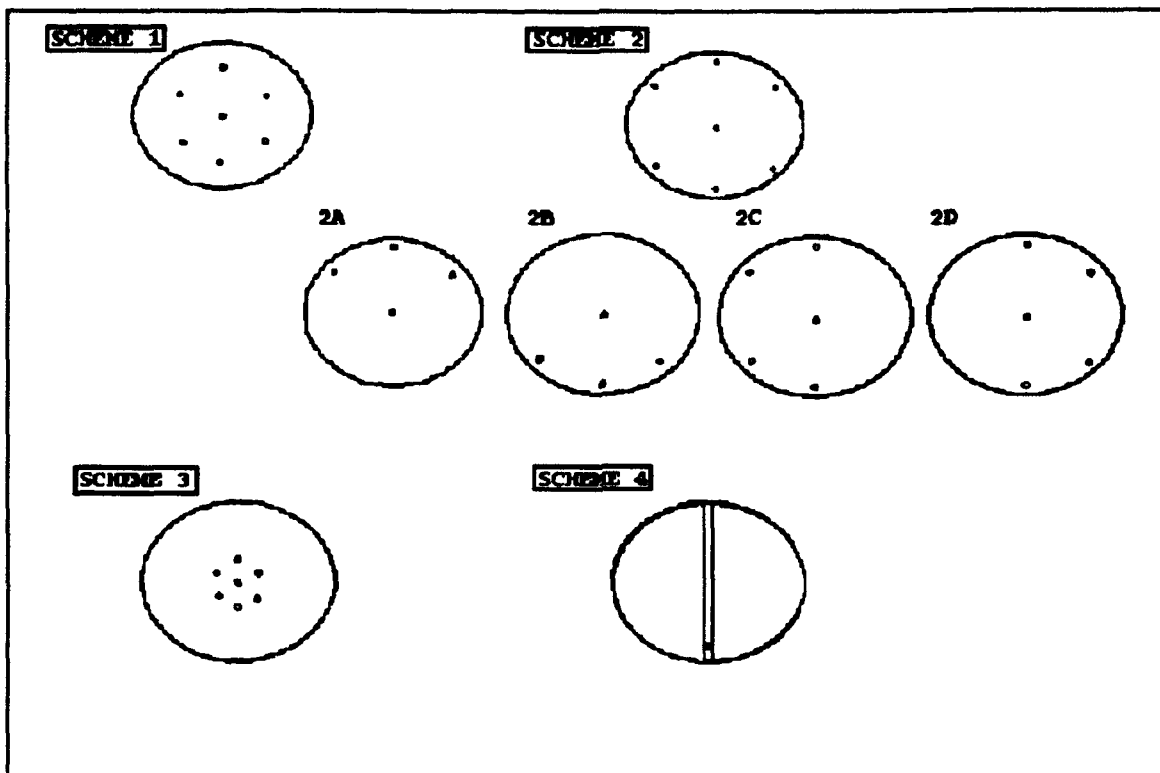


Figure 2.5: Plexiglas Combustor-Model Configurations

motor. The configurations were attached with flanges to the head dome, exhaust, fuel-injector manifold(s) and PVC piping. No exhaust nozzle was used. The combustor/inlet area ratio ( $A_3/A_2$ ) was made identical to that of a combustor in use at the Naval Air Warfare Center Weapons Division, (Airbreathing Propulsion Section), China Lake, CA. A common combustor-dome section and exhaust section were interchanged with center sections having different side-dump geometries. The combustor dome had a variable length ( $L_d$ ) up to 3.5 combustor diameters (D). Configuration 1 was the baseline configuration. It was a single-circular-inlet, side-dump combustor with an area ratio of 1.69. Configuration 2 was a dual-circular-inlet,

side-dump combustor, with inlet dumps circumferentially separate by 90°, and had a combined area ratio of 1.72. Configuration 3 was a dual, axially-in-line, circular-inlet, side-dump combustor, with a combined area ratio of 1.72, and a length between dump planes fixed at four inches (1.2 D). "Fuel" injection was simulated using a seven-injector manifold in which the radial and circumferential positions could be varied. In addition, the number of injectors operating at any time could be varied. The "fuel" was injected in a plane fixed 2.0 inches (0.8 inlet diameters) upstream of the point where the bottom of the inlet side dump interfaced with the combustion chamber. Air or dye was pumped to the injectors using rubber tubing. The "fuel" injection rate was controlled by "needle" valves. "Fuel" injection schemes used for testing are indicated in Figure 2.6. The injector manifold consisted of a 2.0 inch long circular Plexiglas cylindrical section, with flanges at each end to facilitate interfacing between the PVC piping and the model inlet. Each manifold was equipped with seven fittings that held 0.0625 inch brass tubing with an inner diameter of 0.03 inches. The tubing exit was modified to provide small air bubbles or fine dye streams. The brass tubes were introduced normal to the flow and the ends were bent 90° in order to inject dye or air bubbles parallel to the flow. Also, a single 0.125 inch diameter injector was fabricated with ports drilled along the longitudinal axis of the injector to simulate injection from a fuel injector strut.



**Figure 2.6:** "Fuel" Manifold and "Fuel" Injections Schemes

#### B. FLOW-VISUALIZATION EXPERIMENTAL PROCEDURES

Non-intrusive, qualitative analysis of the flow within the three different geometric combustor configurations was accomplished using laser illumination of tracer particles, which simulated injected "fuel" (air bubbles/dye), in water, which simulated the inlet "air" flow. The overall flow field dynamics, major structures, and general mixing quality for each combustor configuration, were analyzed using extensive observation of the changes caused by discrete variations in three parameters. This facilitated the identification of the

combustor geometric configuration that provided the most stable, structurally-uniform, and well-mixed flow field. The parameters varied were dome length, fuel-injection scheme and the "air" mass-flow rates, for the dual-in-line, side-dump combustor. Specific items examined qualitatively to characterize the flow dynamics included, but were not wholly limited to, the relative magnitude and direction of the local time-averaged, two-dimensional velocity, as indicated by tracer streaks, and the intensity of velocity variations, or relative steadiness, of the flow. The major flow-field structural features, symmetric properties, and uniformity were determined using streak lines and dye streams. The general mixing quality of a configuration was determined by assessing the volumetric distribution of tracer particles, or dye, in the flow field, as the parameters were varied.

A reference coordinate system shown by Figure 2.7 was established to conduct testing, aid in the discussion of the results, and to facilitate data reduction. The longitudinal zero reference point was located in the plane of the upstream edge of the forward inlet side dump where it interfaced with the combustion chamber. Positive direction was downstream along the Y axis. However, since all dome-length variations were only in the negative longitudinal direction, they were reported as the positive fraction of combustor diameter (D), with greater dome lengths further in the negative longitudinal direction. The lateral zero-reference point was located at

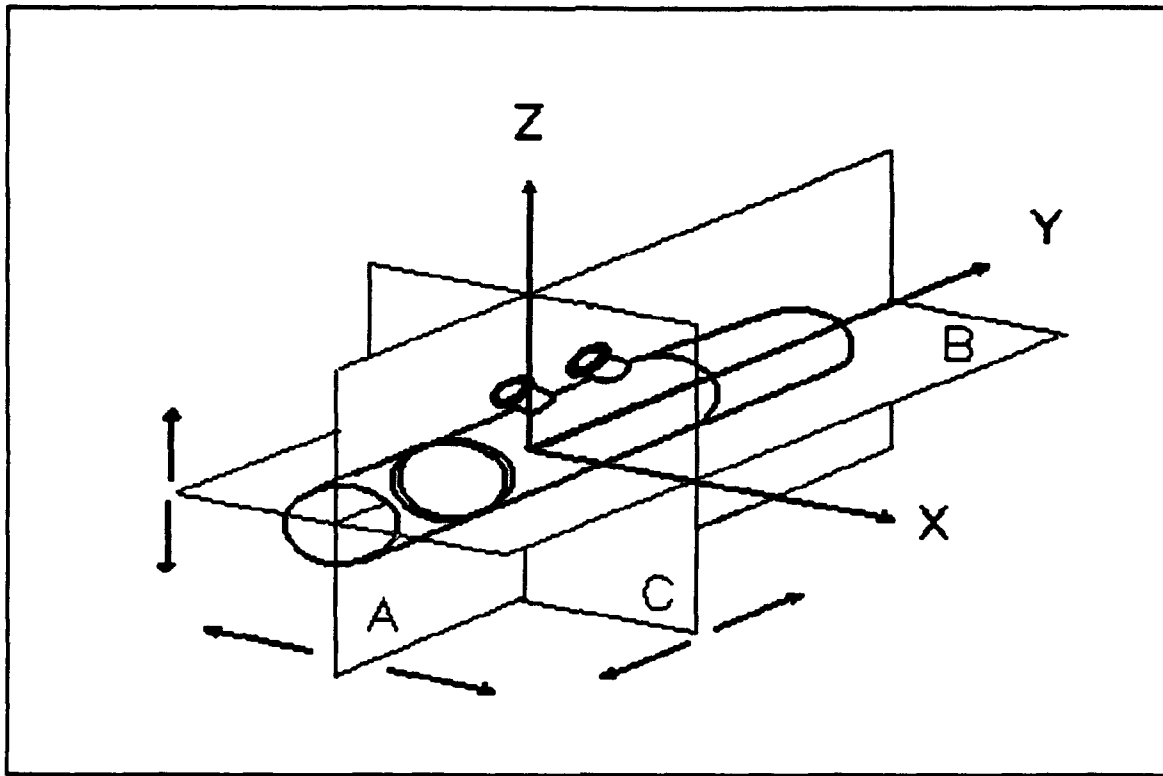


Figure 2.7: Reference Coordinate System

the centerline of the combustion chamber cross section. Positive direction was to the right, along the X axis when viewed from the dome or upstream end. The vertical zero reference point was also located at the centerline of the combustion chamber cross section, with the positive direction along the Z axis toward the inlet on the combustion chamber top. Plane A was the longitudinal plane defined by the Y-Z axes. It represented a laser sheet oriented in the Z direction, with the width of the sheet along the Y axes. Plane B was the lateral plane defined by the X-Y axes. It represented a laser sheet oriented in the X direction, with the width of the sheet along the Y axis. Plane C was the

vertical plane defined by the X-Z axes. It represented a laser sheet oriented in the Z direction, with the width of the sheet along the X axis. Clockwise rotation about the combustion chamber center was considered positive when viewed from the dome, or upstream end of the combustion chamber. The "bottom" of the inlet-side-dump was defined as the most upstream point on the inlet ellipse where the inlet first intersected the combustion chamber. The inlet-side-dump "top" was identified as the most downstream point where the inlet ellipse intersected the combustion chamber. A line connecting these two points was used to establish left and right sides of the inlet when the ellipse was viewed from upstream in the inlet.

The use of similar geometry and operation at similar Reynolds number ensured that the flow field was representative of the flow of an actual, sub-scale ramjet combustor. Air compressibility effects were neglected since the flow field in the actual combustor is nearly incompressible. This enabled the identification of general trends in the model flow behavior that could be expected in the actual combustor. The Reynolds number at the combustor exit for all three configurations was held constant at approximately  $1.07 \times 10^5$ . This was based on an average flow capacity of 110 gpm, which yielded a mass-flow rate of  $15.3 \text{ lb}_m/\text{s}$ . This corresponded to a mass flow rate of air in a sub-scale ramjet of  $0.4 \text{ lb}_m/\text{s}$ . The total inlet "air" mass-flow rate for the single-inlet,

side-dump and the dual-inlet, 90° circumferentially-separated, side-dump combustors, was held constant at  $15.3 \text{ lb}_m/\text{s}$  for the majority of testing. Limited data were collected however, for an inlet mass flow rate of  $0.2 \text{ lb}_m/\text{s}$ , for the single-inlet, side-dump combustor-model. The impact of varying the mass-flow rate of the inlet "air" between the dual inlet in-line side dumps was fully investigated. The mass flow rate of the second inlet was restricted with a gate valve, and the difference in flow rates between inlets was determined from flow-meter readings in the second inlet (downstream inlet). Mass-flow rate percentages used between the first (upstream) and the second (downstream) inlets were 50/50%, 60/40%, 75/25%, 85/15%, and 100/0%.

"Fuel" injection was simulated with water colored dye and air bubbles. Ideally, it was desirable to have small, spherical tracer particles that were neutrally buoyant and as close to the density of water as possible [Ref. 13]. This would insure that the tracer particles followed the fluid. Although water-colored dye particles would generally be good tracer candidates, they were not well suited for showing the flow field in turbulent flows since they tend to mix rapidly. However, this characteristic was ideal for showing the dispersion of injected fuel as well as indicating mixing and non-mixing areas. Water-colored dye was used to analyze the dimensions of the recirculation zones, flow impingement on the combustion chamber's lower wall, and reattachment point(s) of

the flow, as well as to identify general mixing zones. Air bubbles, although not neutrally buoyant or similar in density to water, if small enough would reasonably follow the flow for short periods of time, allowing a qualitative analysis of the flow field. Air bubbles were used to show the flow-field structural patterns, and the degree of mixing of the flow.

"Fuel" injection mass-flow rates were held constant during the flow visualization study. "Fuel" injection was investigated using the injection schemes of Figure 2.6. The impact on the distribution of fuel in the upstream and downstream regions were evaluated by moving the injectors from the inlet-side-dump wall toward the center of the side dump. Single operating injectors, as well as multiple injectors operating simultaneously, were evaluated for their impact on fuel distribution.

Dome length ( $L_d$ ) was varied for all configurations from the longitudinal zero reference point to 3.5 D (-11.4 inches). Detailed data were collected for dome lengths up to 1.2 D (-4.0 inches) in increments of 1.0 inch. For each increment of dome length the laser sheet was repositioned laterally, longitudinally, and axially in the combustor model in order to investigate the local two-dimensional flow conditions throughout the flow field. For each increment of dome length, the laser sheet was positioned at 0,  $\pm 1.0$ , and  $+ 1.5$  inches in the lateral ( $L_{lx}$ ) or X direction. Similarly, the laser sheet was positioned in the vertical ( $L_{lz}$ ) or Z direction at

0,  $\pm 1.0$ , and -1.5 inches, for each increment of dome length. The laser sheet was also positioned axially ( $L_{1y}$ ), illuminating circular cross sections of the combustion chamber. The sheet was moved longitudinally, at one inch increments, from the dome's position, in order to view the flow field cross section.

Time-elapsed photographs of the tracer particles were taken by setting the 55mm SLR camera at a slightly oblique angle, in the direction of the forward scattered laser light, rather than normal to the laser sheet. The camera was set at 1/30 second shutter speed to provide streak images of illuminated tracer particles. Also, annotated high resolution video was taken to provide a record of near-real-time flow conditions of the laser-illuminated particles, as well as the particles illuminated with ambient light.

### III. RESULTS

The flow-visualization results for each combustor configuration are sub-divided into four parts. The first part is a general description of the flow-field structure and dynamics. The second part includes an analysis of the impact of discrete changes in the dome length on the mixing characteristics and stability within the flame-holding or dome region. The optimum dome length for each configuration is identified. Conditions were considered optimum if there were no flow instabilities evident and the tracer particles were well mixed in the region. The third part is an analysis of the impact of changes in dome length on mixing quality in the main combustion region. Conditions were again considered optimum when tracer particles were uniformly mixed and no flow instabilities were evident. The fourth part includes an analysis of the impact of changes in inlet "fuel" injection location on the expected flammability in the flame holding region, and the expected combustion efficiency (mixing) in the main combustion region. Locations within the inlet(s), to assure optimum distribution for flame stability and combustor mixing, are identified. "Fuel" distribution was considered optimum when the "fuel" was distributed both uniformly and steadily into the region. Additionally, a comparison of the results of this flow-visualization investigation of three

geometries is made with other similar studies reported in the literature.

In general, the photographic data from the flow visualizations were considered adequate to obtain the desired mixing and stability information, even though non-ideal tracer particles were used. The tracer streaks that resulted from the time-elapsed photography showed that in the region of the inlet center (where particle motion was nearly two dimensional and the flow well developed) the particles had velocities close to the calculated one-dimensional velocity (-6%) based on flow-rate measurements made slightly upstream of the inlet.

#### A. SINGLE-SIDE-DUMP COMBUSTOR

##### 1. General Flow Field Structure

The flow can be characterized by three regions, as shown in Figure 3.1; the dome region (flame holding region) located upstream of the inlet side dump, the jet-inflow and impingement region, and the main-combustion region located downstream of the inlet side-dump.

###### a. The Dome Region

The dome region was defined in the longitudinal direction by the inlet-jet streamtube and the adjustable dome. The dominant characteristic of the flow was a circulation structure in the longitudinal plane of the region located at the center of the combustion chamber. The relatively high velocity inlet-jet, and relatively stationary (initially)



**Figure 3.1:** Configuration 1 in Operation in the Water Tunnel

fluid in the dome region, generated shear stresses. The resulting vortices, and the fluid motion generated from the inlet jet impinging on the lower combustor wall and then moving into the dome region along the combustor wall, were responsible for this longitudinal circulation pattern. Figure 3.2 shows the typical flow field observed in the longitudinal plane of the dome region. Also, note the indication of flow moving normal to the longitudinal plane, as indicated by points of reflected light near the dome at the top and bottom of the combustion chamber. Figure 3.3 (laser sheet in the lateral (B) plane), also showed the dominant longitudinal direction of flow at the center of the combustion chamber as viewed from below the recirculation zone. Again, note that as

the flow moved away from the combustor center it gradually became normal to the longitudinal axis. This movement of the flow circumferentially around the combustor wall is also shown in Figures 3.4 and 3.5 as the laser sheet was translated in the longitudinal (A) plane away from the centerline. These figures indicated the existence of two additional flow structures in the dome region. First, the flow near the dome rotated clockwise about the axial centerline of the combustor, as shown in Figure 3.6. Second, along each side of the combustion chamber the flow moved out of the region in two counter-rotating patterns, as shown by Figure 3.7. The transition between these patterns became evident as the laser sheet in the vertical (C) plane was translated in the direction of the positive Y axis. The flow transitioned from the clockwise rotation into two large counter-rotating circulation patterns along the combustor wall near the same location that the longitudinal circulating structure was observed. The counter-rotating patterns decreased in size (became more tightly wound), and moved downward as the laser was translated toward the inlet jet stream. This result was attributed to a constriction of all three streamtubes (pinching effect) by the inlet flow. Additionally, at longer dome lengths, a vortex pattern developed along the center of the combustion chamber in the dome region. The vortex was generally attached to the dome in the upper left semi-circle, and vacillated in the left half of the flame-holding region

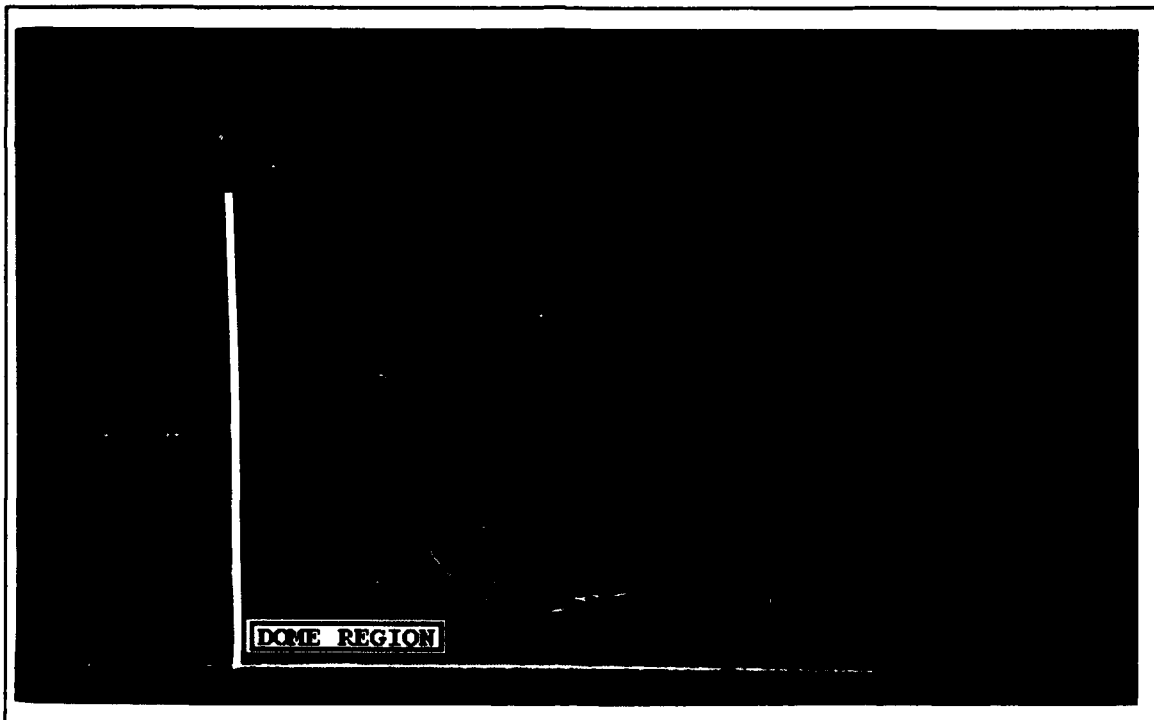


**Figure 3.2:** Configuration 1; Dome Region,  $L_d = -1"$ ,  $L_{lx} = 0"$

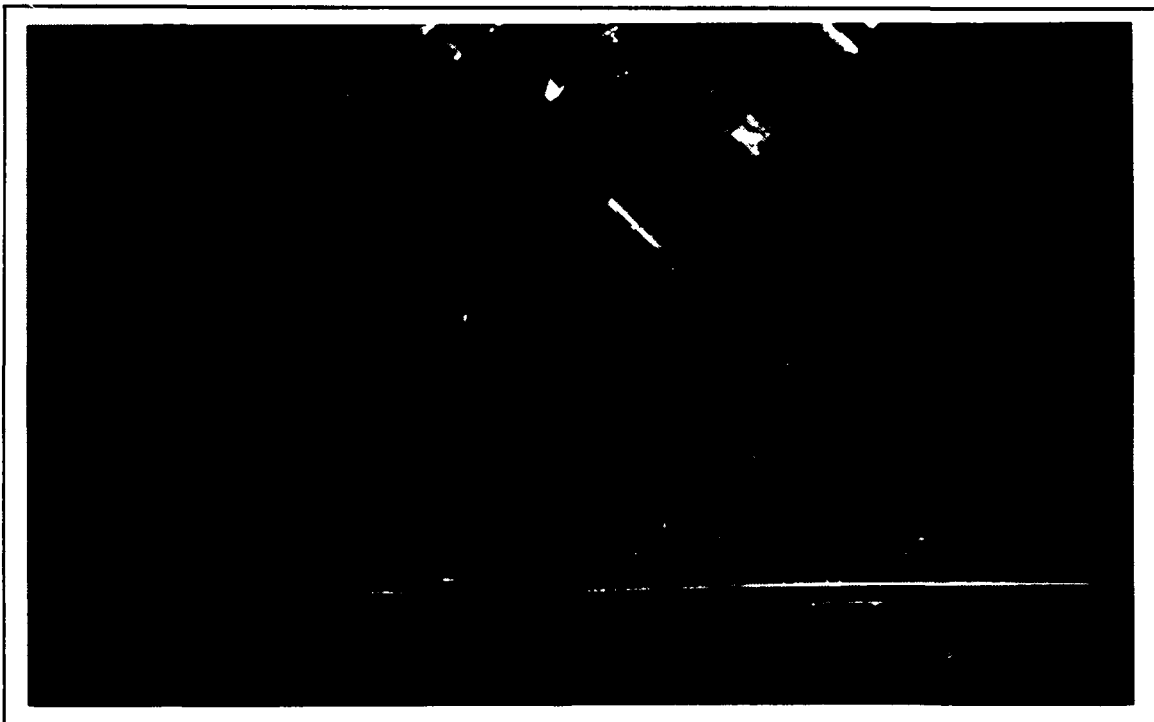


**Figure 3.3:** Configuration 1; Dome Region,  $L_d = -1"$ ,  $L_{lx} = 1"$

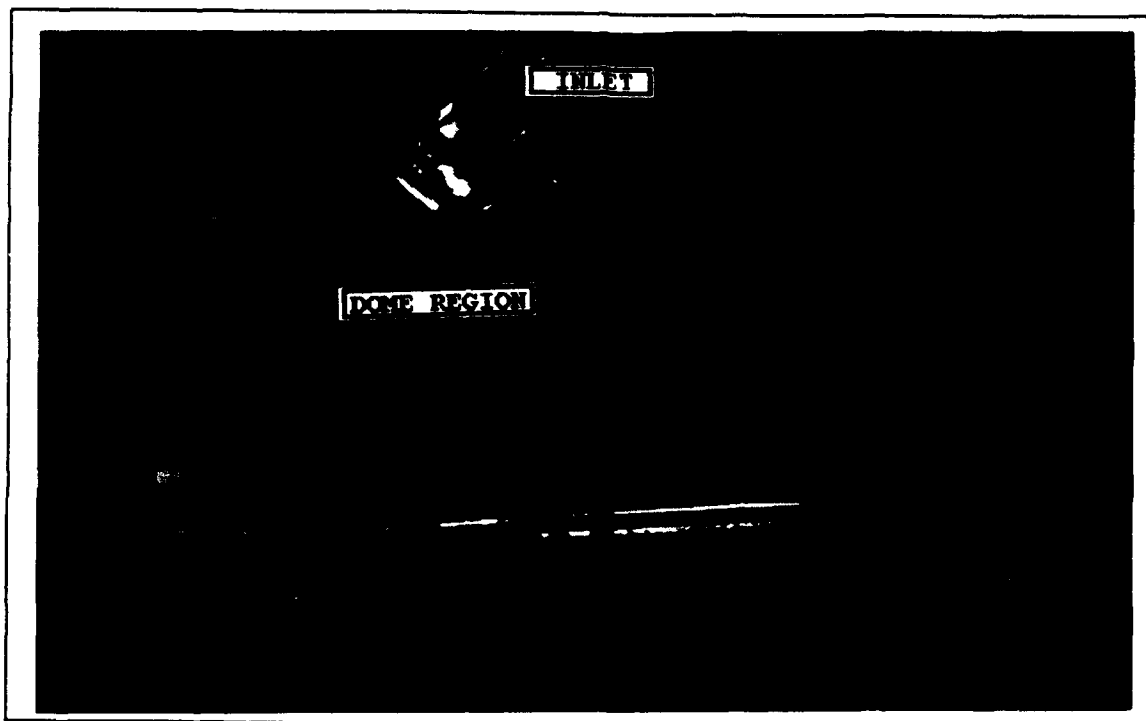


**Figure 3.4:** Configuration 1; Dome Region  $L_d = -1"$ ,  $L_{1z} = 1"$

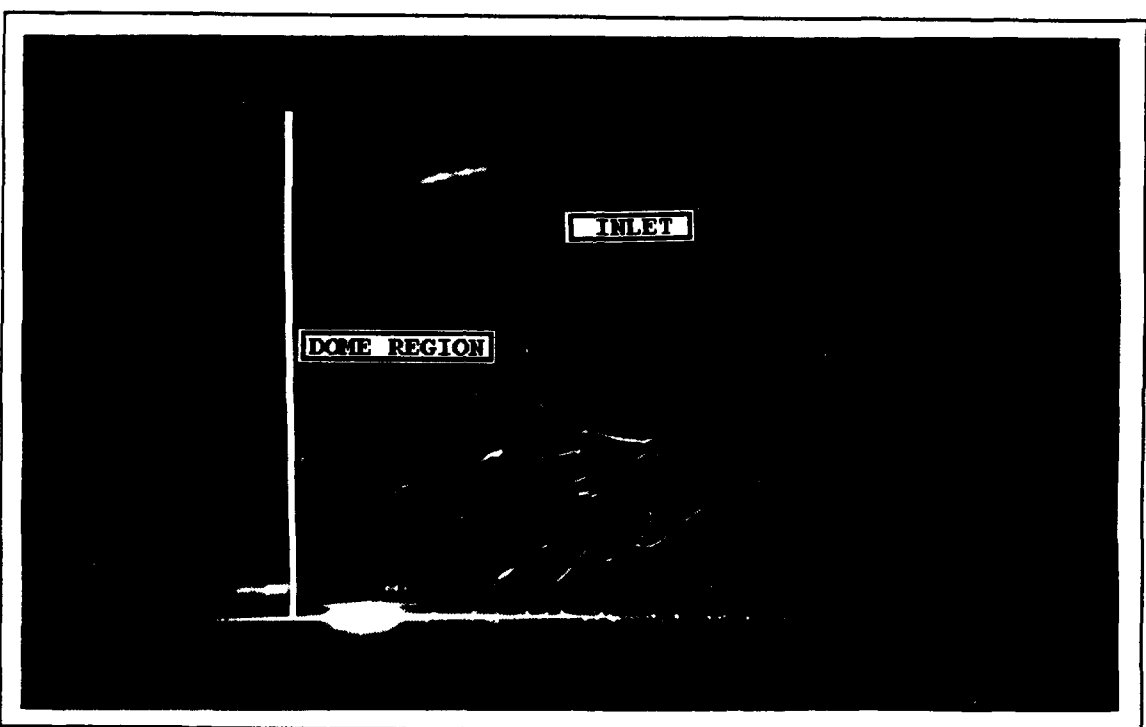


**Figure 3.5:** Configuration 1; Dome Region  $L_d = -1"$ ,  $L_{1z} = 1.5"$



**Figure 3.6:** Configuration 1; Dome Region,  $L_d=-4"$ ,  $L_{ly}=.5"$

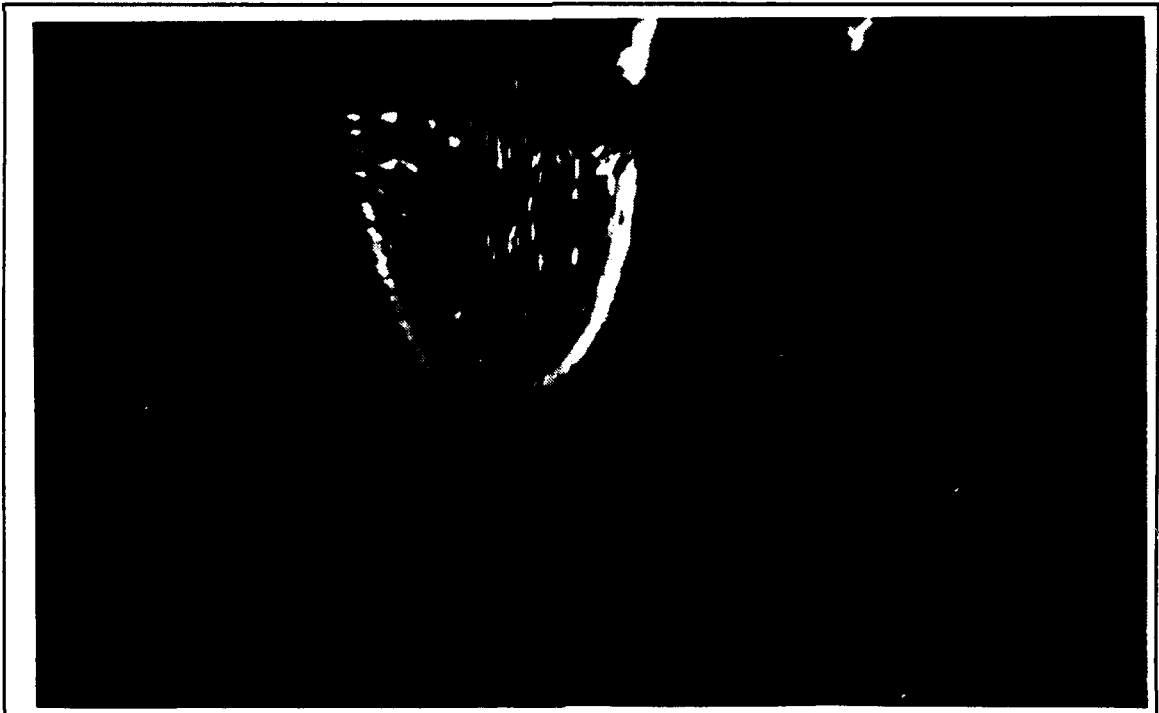


**Figure 3.7:** Configuration 1;  $L_d=0"$ ,  $L_{ly}=1"$

extending longitudinally along the combustion chamber. It crossed the centerline at the approximate location of the observed longitudinal circulation pattern as shown in Figure 3.8.

***b. Inlet-Jet Expansion and Impingement Region***

The inlet-jet impingement streamtube constituted a region extending from the inlet interface with the combustion chamber at approximately  $45^\circ$ , to the lower combustor wall. There, a jet spreading of nearly 2.0 inches resulted in an impingement region which measured from approximately  $0.77 D$  to approximately  $1.85 D$  downstream of the zero longitudinal reference point. The jet impingement point (center of

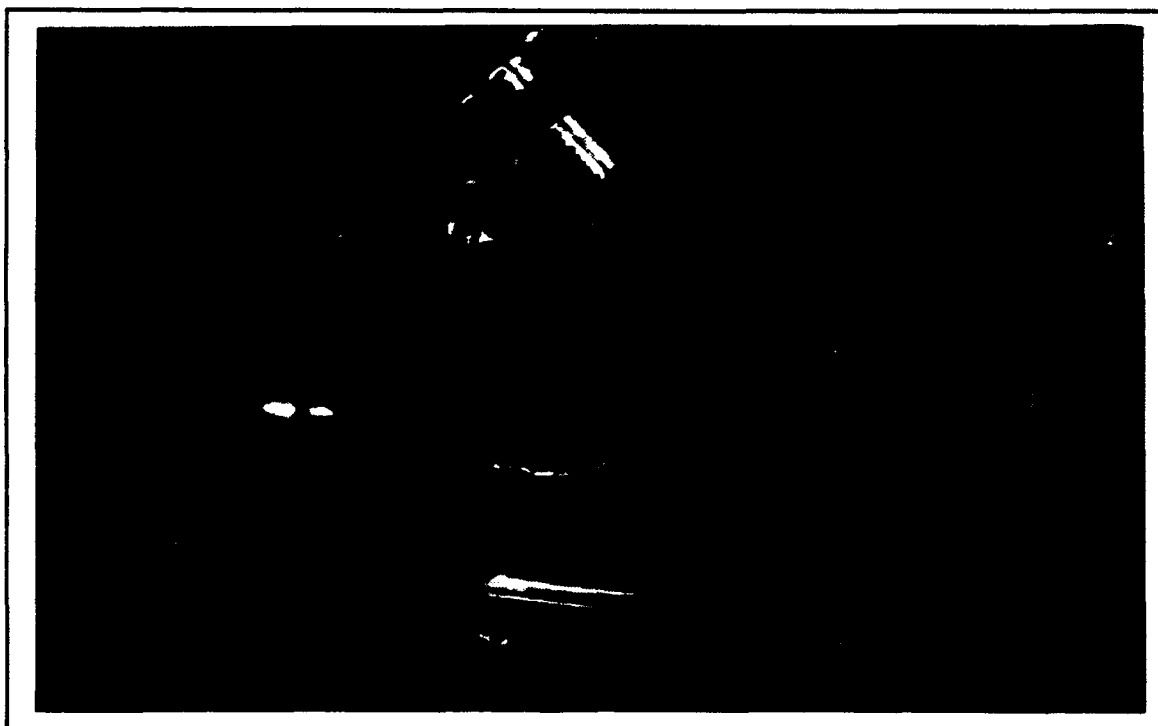


**Figure 3.8:** Configuration 1; Dome Region,  $L_d = -4$ ,  $L_{1z} = 0$

impingement jet) was located on the combustor wall approximately 1.2 D from the zero longitudinal reference point. The point where the impinging streamtube flow clearly separated between the dome region and the region downstream, was located 0.77 D from the longitudinal zero reference point. The inlet streamtube was also pinched by the counter-rotating flows exiting the recirculation zone on each side of the combustor, as discussed above.

### c. Main Combustion Region

As the flow moved downstream it divided into two counter-rotating streamtubes located on each side of the combustion chamber. These streamtubes flowed around the inlet streamtube, and as a result began to twist about the combustor centerline. The left streamtube twisted down while the right streamtube twisted up. These streamtubes and the inlet streamtube began to wrap around each other, contracting in the process, and eventually coalescing into one swirling streamtube. The contraction of the flow in the initial turns of the twisting streamtubes was evident at 2.15 D downstream of the longitudinal zero-reference point. After the initial turn, the flow expanded to occupy the entire combustion chamber at approximately 2.77 D. The flow just downstream of the inlet side dump exhibited a cross flow pattern where the structural integrity of the counter-rotating streamtubes diminished due to the influence of the inlet jet. Figure 3.9

is a photograph of the flow field illuminated in the axial plane that shows the lazy S pattern distinctive of this flow characteristic. Again, at approximately 2.15 D, this pattern dissipated into a pattern were uniform flow rotating clockwise was clearly evident.



**Figure 3.9:** Configuration 1; Main Combustor,  $L_d = -4"$ ,  $L_{ly} = 3.5"$

**2. Impact of Dome Length ( $L_d/D$ ) on Flow Stability and Mixing in the Dome and Main Combustion Regions**

**a. The Dome Region**

The dome region (flame-holding region) exhibited generally unsteady flow characteristics. However, the relative stability and steadiness of the flow was improved for

particular ranges of dome length. Significant changes to the dominant flow-field structure occurred as the dome length was varied. In addition to the dissipation of the longitudinal circulation structure, as evidenced by a looser circulation pattern, the center of this circulation pattern clearly moved in the negative longitudinal direction as dome length was increased. Figure 3.10 shows the measured position of the center of the longitudinal circulation pattern as the dome length was varied. For dome lengths shorter than 0.5 D, the entering and exiting mass flows periodically became unstable. Also, as a result of the surging nature of the mass flow in the dome region with short dome lengths, the inlet jet wavered laterally in synchronization. This phenomenon dissipated and was not observed when the dome length was increased beyond approximately 0.54 D. As the dome length was increased, the mass flow into and out of the zone balanced, and the flow returned to a steady recirculating pattern. Dome lengths between 1.1 D and 1.5 D resulted in a relatively stable vortex pattern in the recirculation zone, but resulted in poor mixing. The optimum dome length for this configuration was between 0.5 D and 1.1 D, since it provided the most stable flow pattern (no vortex shedding) with generally good mixing, and thus potentially adequate flame stability.

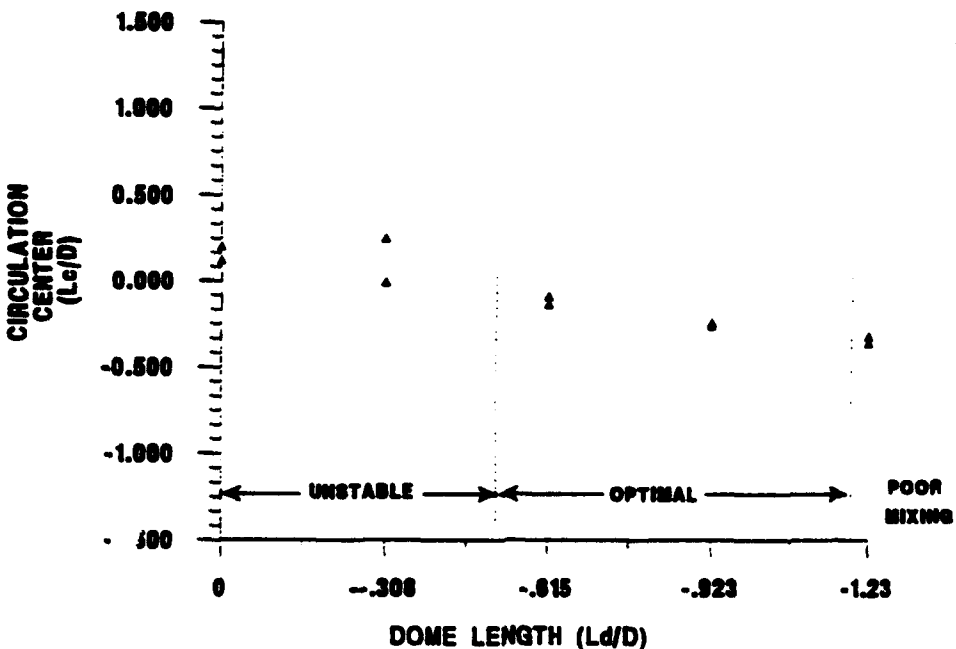


**Figure 3.10:** Configuration 1; Longitudinal Circulation Center ( $L_c$ ) Verses Dome Length ( $L_d$ )

#### **b. The Main Combustor Region**

Dome length had no significant affect on the stability and mixing in the main combustion region downstream of the inlet side dump except for dome lengths less than 0.5 D. At these short dome lengths, the entire flow field would periodically accelerate momentarily, due to the oscillatory mass flow into the flame holding region.

#### **3. Mixing within the Main Combustor**

The degree of mixing was the primary criterion utilized for determining when the main combustion region could be expected to provide good combustion efficiency. The mixing quality was analyzed by qualitatively assessing the percentage

of the combustor volume occupied by tracer particles in the zone, and identifying regions of tracer particle concentration. Generally, the percentage of combustor volume occupied increased with distance from the longitudinal zero reference point as the flow reattached to the combustor wall. This can be attributed to the twisting structure of the three streamtubes entering the combustor as discussed above. Between 0.9 D and 2.15 D downstream of the inlet, the flow remained separated between the three streamtubes. The percentage of volume of the combustion chamber occupied by tracer particles experienced an approximate decrease of 25 percent in this area. At approximately 2.15 to 2.77 D, the streamtubes clearly intermingled into one swirling streamtube, with nearly 100 percent of the volume occupied by particles beyond 2.8 D.

#### 4. "Fuel" Injection Pattern Impact on "Fuel" Distribution

A steady "fuel" distribution in the flame holding region and a steady and uniform distribution in the main combustor region are generally desired to ensure flammability and efficient combustion. The effects of changes in both the circumferential and radial positions of "fuel" injection within the inlet duct were measured for each dome length. Figure 3.11 summarizes the results for the impact of "fuel"

injection location on "fuel" distribution in the flame-holding and main combustion regions.

*a. Impact of "Fuel" Injector Location on "Fuel" Distribution in the Dome/Flame-Holding Region*

"Fuel" injection from the bottom one sixth of the inlet cross sectional area steadily and uniformly distributed "fuel" into the flame-holding region. Injectors 3, 4, 5, and 6 provided the best distribution of fuel into the dome region. Injector 5, on the bottom of the inlet wall, provided the most steady and uniform "fuel" distribution into the dome region of these four injectors. Changing the location of "fuel" injection position from  $180^\circ$  to less than  $135^\circ$  or more than  $225^\circ$ , had the affect of reducing the "fuel" flow into the dome region. The remainder of the "fuel" was distributed downstream. For circumferential positions above  $135^\circ$  and  $225^\circ$ , "fuel" was not distributed steadily into the dome region. This area along the left and right inlet sides distributed "fuel" into the counter-rotating vortex patterns leaving the dome region.

Varying the distance of the fuel injectors from the inlet-side-dump wall showed that, as the injection point approached the center of the circular dump, both steadiness and uniformity of the distribution deteriorated in the dome region. The best "fuel" distribution was found to be when the "fuel" injector was positioned between 0.7 and 1.0 inlet radii

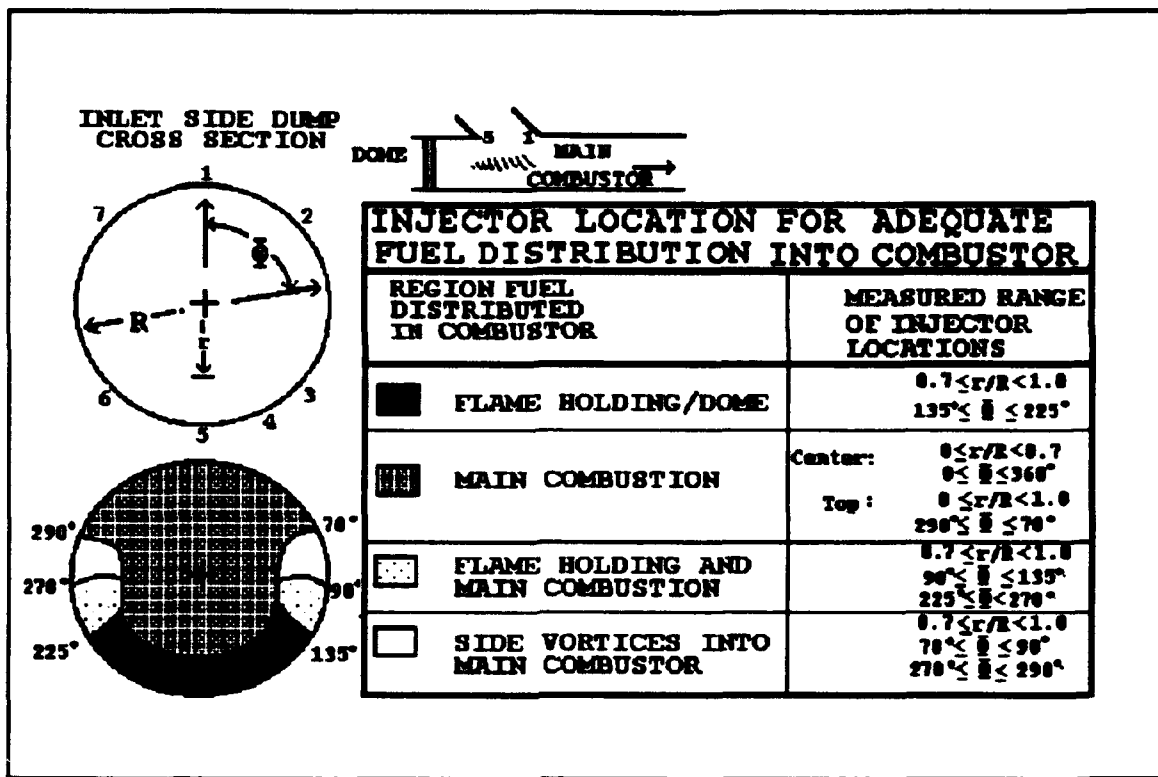


**Figure 3.11:** Impact of "Fuel" Injection Location on "Fuel" Distribution, Configuration 1.

(R) from the centerline of the inlet duct.

Increasing dome length decreased the uniformity of distributed "fuel" into the dome region, but did not affect the distribution steadiness.

**b. Impact of "Fuel" Injector Location on "Fuel" Distribution in the Main Combustion Zone**

As shown by Figure 3.11, "fuel" was distributed into the main combustor region by all injection locations in the center and top of the inlet. However, it was noted that to achieve uniform "fuel" distribution in the main combustor, injection from several locations was required. "Fuel"

injection from the center alone resulted in no "fuel" distribution to a region at the top of the combustor just downstream of the inlet (approximately 0.9 D to 2.15 D). As injection was made closer to the top of the inlet "fuel" was distributed more adequately into this region, but little "fuel" was distributed along the bottom of the main combustor. Also, "fuel" injection along the left and right sides of the inlet clearly fed the side vortices moving around the inlet jet. Thus, to achieve a steady and uniform "fuel" distribution into the main combustor, multiple injector locations in the inlet should be used.

**B. DUAL-INLET SIDE-DUMP COMBUSTOR WITH INLETS SEPARATED BY  
90°**

**1. General Flow-Field Structure**

Similarly to the single-side-dump combustor, the flow field could be divided into three rather distinct regions; a dome/flame-holding region, a jet-inflow and impingement region and a main-combustion region. The two inlets resulted in a remarkably similar flow structure to the single side dump but the dynamics were quite different.

**a. Dome/Flame-Holding Region**

The flame-holding region could be defined longitudinally by the head-end of the dome and the intersection of the flow of the two inlet jets. The entering streamtubes impinged upon each other approximately 0.46

combustor radii directly above the combustor centerline, at approximately 0.32 D [Figures 3.12 and 3.13]. As a result of the jet-on-jet impingement, the flow became nearly two dimensional with a sheet of fluid impinging on the lower combustor wall, as seen in Figure 3.14. This behavior also resulted in a longitudinal recirculation region, as shown in Figure 3.15. A central vortex also formed in the dome region for nearly all dome lengths. This occurred as the longitudinal recirculation pattern weakened (when moving into the dome region). Thus, the jet-on-jet impingement generally weakened the longitudinal recirculation pattern, which in turn permitted the vortex formation. The formation of counter-rotating vortices, which exited the dome region, was also observed. However, the two-dimensional jet sheet resulted in less distortion of the counter-rotating structure than was observed for the single-side-dump combustor. As the flow moved downstream passed the inlet, the "pinching" effect was not as prominent.

#### *b. Jet Impingement Region*

The flow field structure and dynamics in the jet impingement region were considerably different from the structure and dynamics observed in the single-side-dump configuration. The jet-on-jet impingement, and radial distribution of fluid from the impingement point (Figure 3.15) reduced the expansion of the inlet flows into the combustor



Figure 3.12: Configuration 2; Top View, Dome Region,  $L_d=0"$ ,  $L_{lx}=1"$

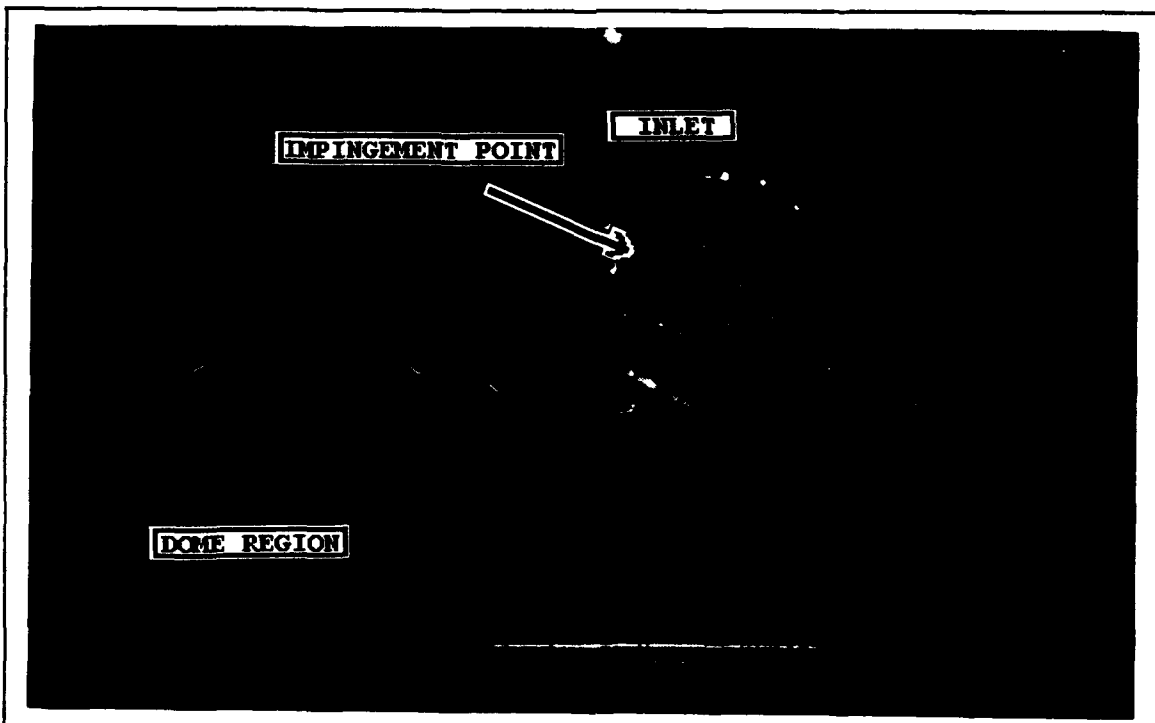
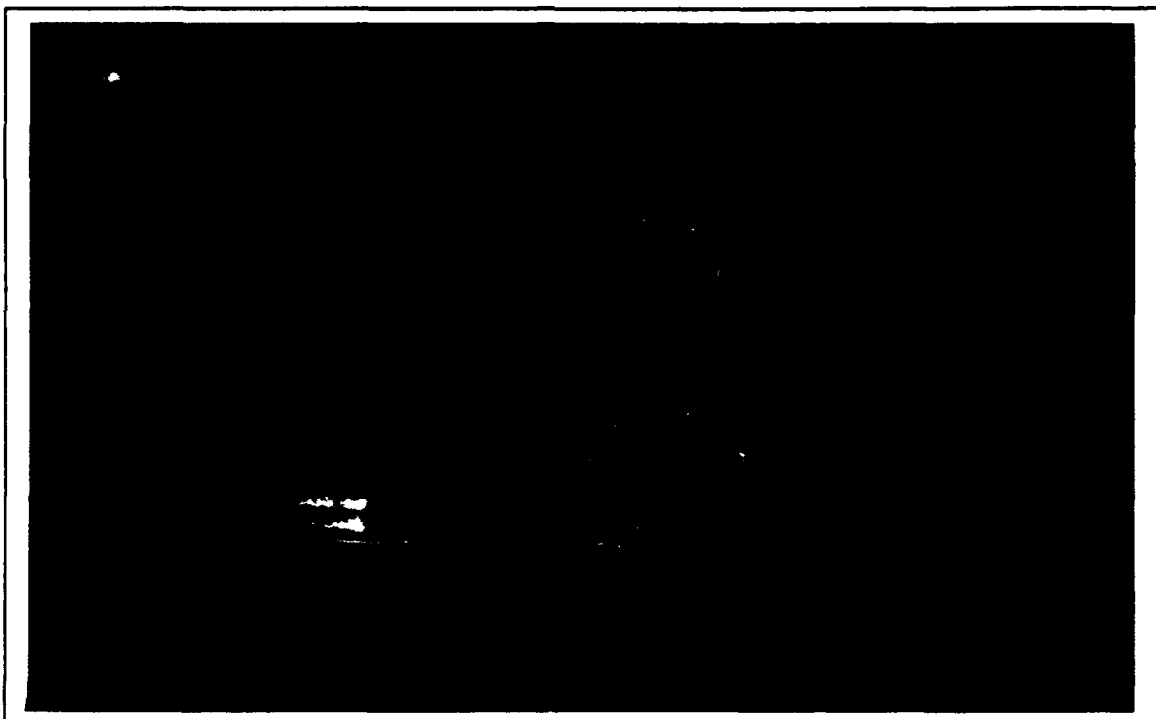
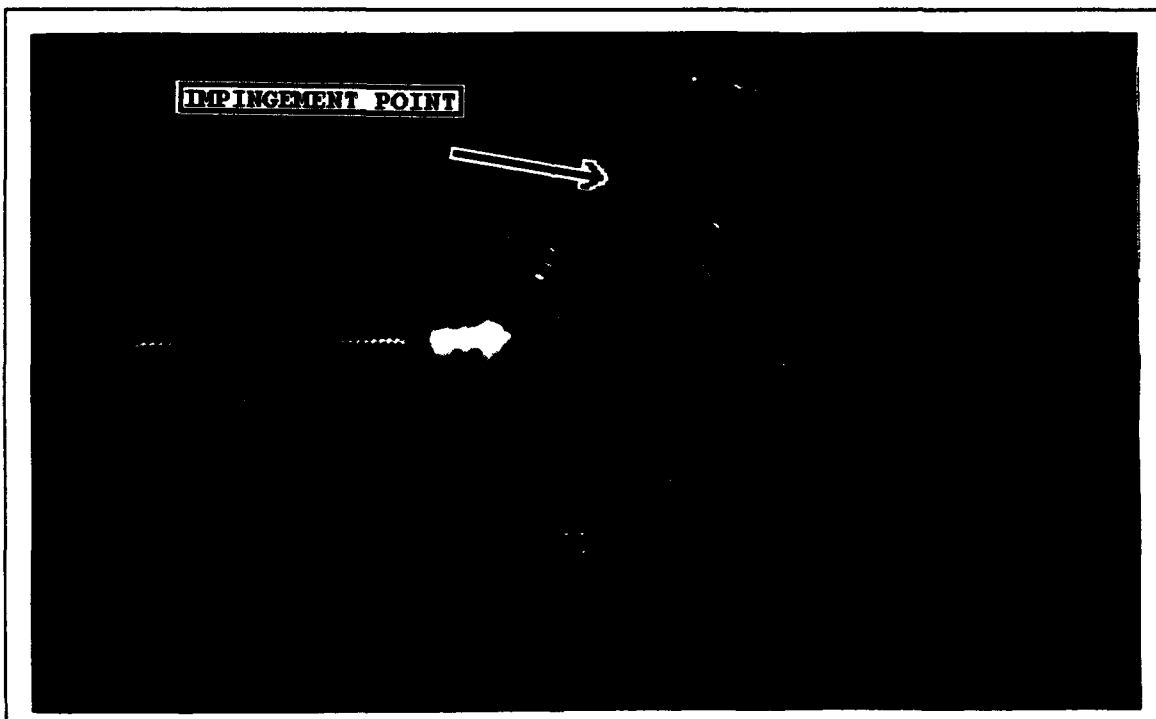


Figure 3.13: Configuration 2; Dome Region,  $L_d=-4"$ ,  $L_{lz}=0"$



**Figure 3.14:** Configuration 2; Bottom View, Dome Region,  
 $L_d=0"$ ,  $L_{1z}=0"$



**Figure 3.15:** Configuration 2; Dome Region,  $L_d=0"$ ,  $L_{1z}=0"$

chamber from that observed in Configuration 1. The sheet impinged on the combustor wall between 0.15 D and 0.73 D. As the flow impinged on the wall it moved in essentially four directions. The flow moved along the Y axis, upstream into the dome region, and downstream into the main combustion region. It also moved circumferentially upward in both directions.

*c. The Main Combustion Region*

This region was composed of swirling streamtubes similar to the single-side-dump configuration. However, the fluid appeared to be less turbulent initially than in the single-side-dump configuration due to the two dimensional structure of the sheet of fluid created by the impinging jets. The region did exhibit the twisting of three streamtubes into one, with a contraction similar to that seen in the single-side-dump configuration. The contraction began at 0.77 D, and diverged to fill the entire chamber at 1.23 D. The pattern shown by the laser sheet passing through the combustor cross section at 1.23 D was swirling but completely uniform.

**2. Impact of Dome Length ( $L_d/D$ ) on Flow Stability and Mixing in the Dome and Main Combustion Regions**

*a. The Dome Region*

The result of the nearly two-dimensional flow pattern (jet sheet), and weaker longitudinal circulation pattern, was the formation of a central vortex in the dome

region for nearly all dome heights. As shown in Figure 3.16, the movement of the center of the recirculation pattern was not clearly in the negative longitudinal direction for different dome lengths, but remained nearly constant as dome length was increased. The only major changes in circulation pattern location occurred when visible instabilities (vortices or vortex shedding) were observed. The dome-length range that provided the optimum flow stability and mixing for this configuration was between 0.31 D and 0.88 D. A stable but weak central vortex formed in the dome region for these dome lengths. Although tracer particles were always concentrated

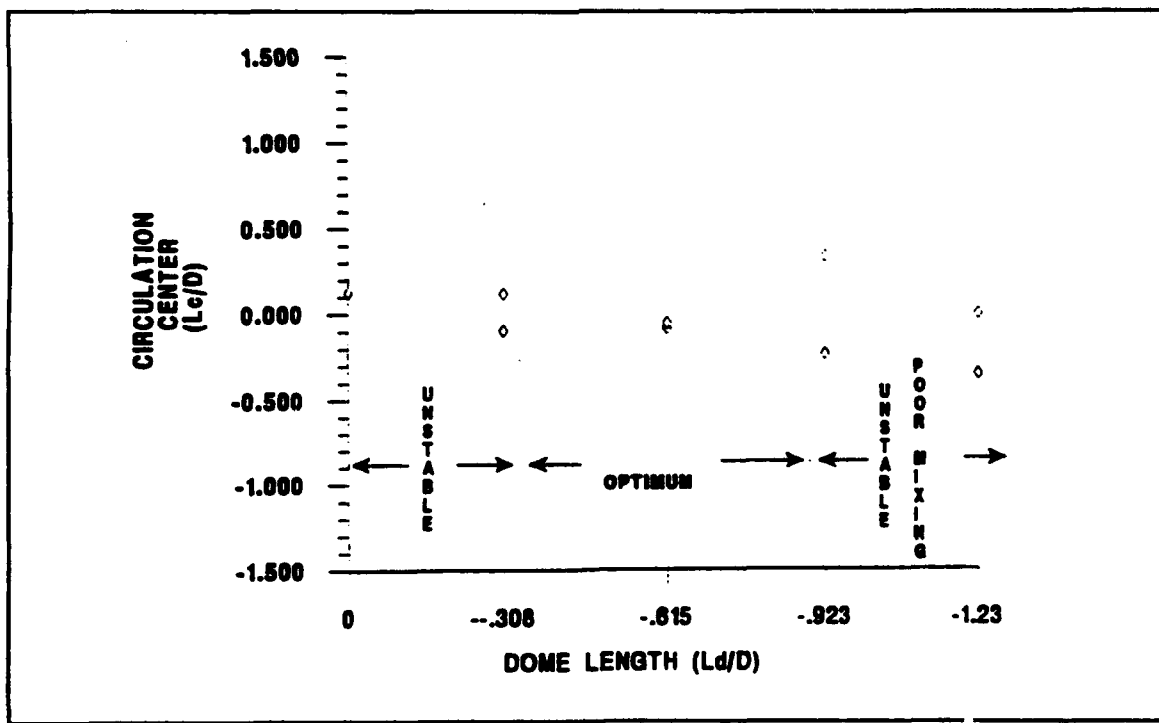


Figure 3.16: Configuration 2; Longitudinal Circulation Center ( $L_c/D$ ) Verses Dome Length ( $L_d/D$ )

in this vortex region, lower concentrations were observed for this range of dome lengths. At dome lengths less than 0.31 D, the flow was unstable, with nearly periodic vortex shedding into the region. At dome lengths greater than 0.88 D, the vortex became intermittent and formed nearly periodically, causing accelerations in the flow. At dome lengths greater than 1.23 D, the mixing quality decreased significantly, with fewer tracer particles reaching the region in the vicinity of the dome.

#### **b. The Main Combustion Region**

The main combustion region remained relatively stable for all dome lengths except for the occurrence of small fluctuations when the dome lengths were less than 0.31 D. As for the single-side-dump combustor, instabilities in the flame-holding region were transmitted to the main combustion chamber by accelerations in the flow in the counter-rotating vortices. However, these fluctuation were not as intense as the fluctuations noted in the main combustion chamber of the single-side-dump configuration.

#### **3. Mixing within the Main Combustor**

The mechanism that facilitated mixing in the main combustion chamber was not noticeably different from that observed in the single-side-dump configuration, but the volume occupied by active mixing was considerably greater. The generation of a fluid sheet in the flow field as a result of

jet-on-jet impingement resulted in a shorter twisting, contraction and expansion of the three streamtubes (inlet jet and two side vortices). This observation implies that more of the combustion chamber would be available for burning of fuel and air, thus an increase in combustion efficiency could be expected. Also, this pattern did not change as dome length was varied.

#### 4. "Fuel" Injection Pattern Impact on "Fuel" Distribution

The structure and dynamics of the flow field had significant impact on the "fuel" distribution in the combustion chamber. Figure 3.17 shows the results of optimizing the "fuel" injection location in the inlets to ensure steady and uniform "fuel" distribution in the flame holding and main combustion regions.

##### a. *Impact of "Fuel" Injector Location on "Fuel" Distribution in the Recirculation/Flame-Holding Region*

As with Configuration 1, the optimum location for "fuel" injection in the inlet of Configuration 2, that insured steady and uniform distribution of "fuel" into the dome region was in the lower zone described in Figure 3.17. Again, as the radial location was moved away from the wall of the inlet, and/or circumferentially away from the bottom of the inlet, less fuel was distributed into the dome region. Also, dome

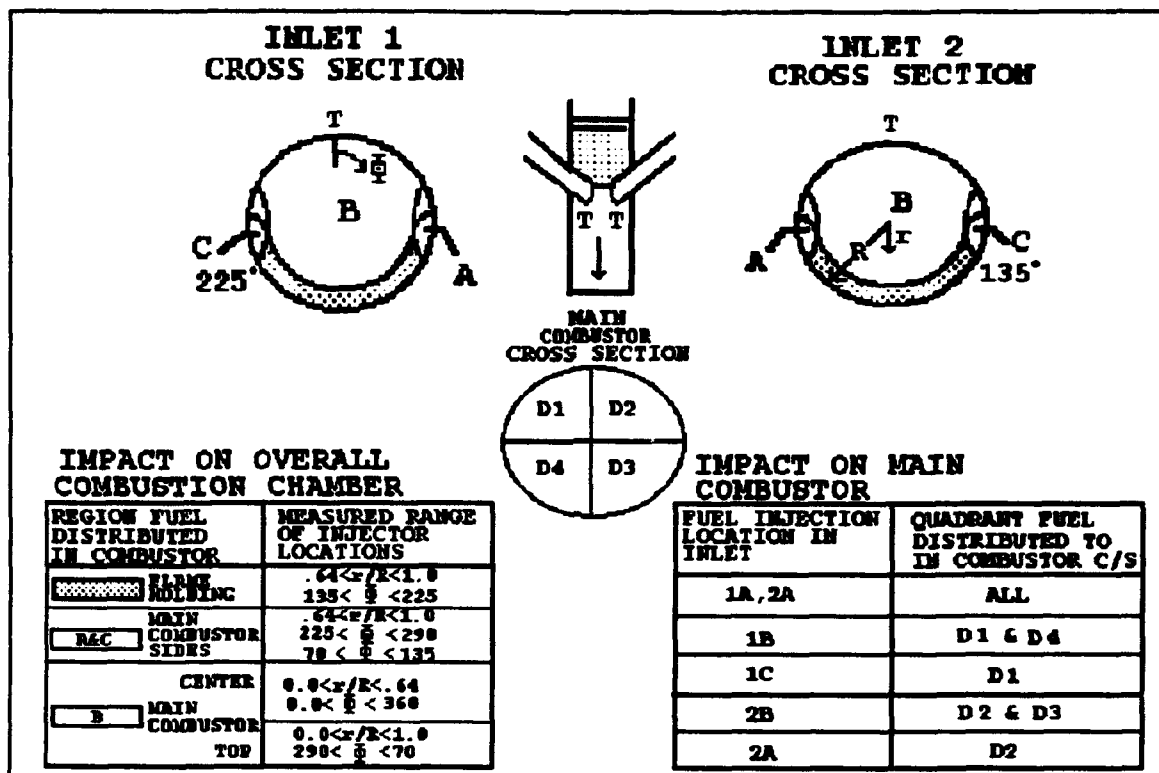


Figure 3.17: Impact of "Fuel" Injection Location on "Fuel" Distribution, Configuration 2

length had no visible influence on the steadiness or uniformity of "fuel" distribution into the dome region.

*b. Impact of "Fuel" Injector Location on "Fuel" Distribution in the Main Combustion Region*

The inner sides (regions 1 A and 2 A in Figure 3.17) of the inlets were the optimum location for "fuel" injectors in order to insure that the "fuel" was distributed uniformly and steadily into the main combustion region. These regions distributed "fuel" into the portion of the inlet jet that moved directly downstream into the cross flow region established by the twisting streamtube. Mixing was immediate

throughout the main combustor. "Fuel" injection into the center of the inlets (regions 1B and 2B of Figure 3.17) tended to be distributed into the left (D1 and D4) and right (D2 and D3) semi-circles respectively of the combustor cross section. At approximately 1.23 D downstream, this "fuel" became well mixed in the combustor region. "Fuel" injected from the outer sides of the inlets (regions 1C and 2C), was initially only distributed into the upper left and right quadrants (D1 and D2) of the combustor cross section, but the "fuel" mixed throughout the chamber at approximately 1.23 D. Thus, although injection from inlet regions 1A and 2 A provided good "fuel" distribution in the main combustor, injection should be made from regions B and C to ensure maximum utilization of the combustion chamber. Varying dome length did not visibly alter these results.

### C. DUAL IN-LINE SIDE-DUMP COMBUSTOR

#### 1. General Flow Field Characterization

The flow field is shown in Figure 3.18 and was comprised of a dome region (region 1), two jet-impingement regions, an additional region of mixing between the inlet jets (region 2, or ancillary combustor region), and the main combustion region (region 3). The dome-region flow-field structure and dynamics closely resembled the single-side-dump combustor flow-field structure and dynamics. However, the ancillary combustion or mixing zone between the side-dump

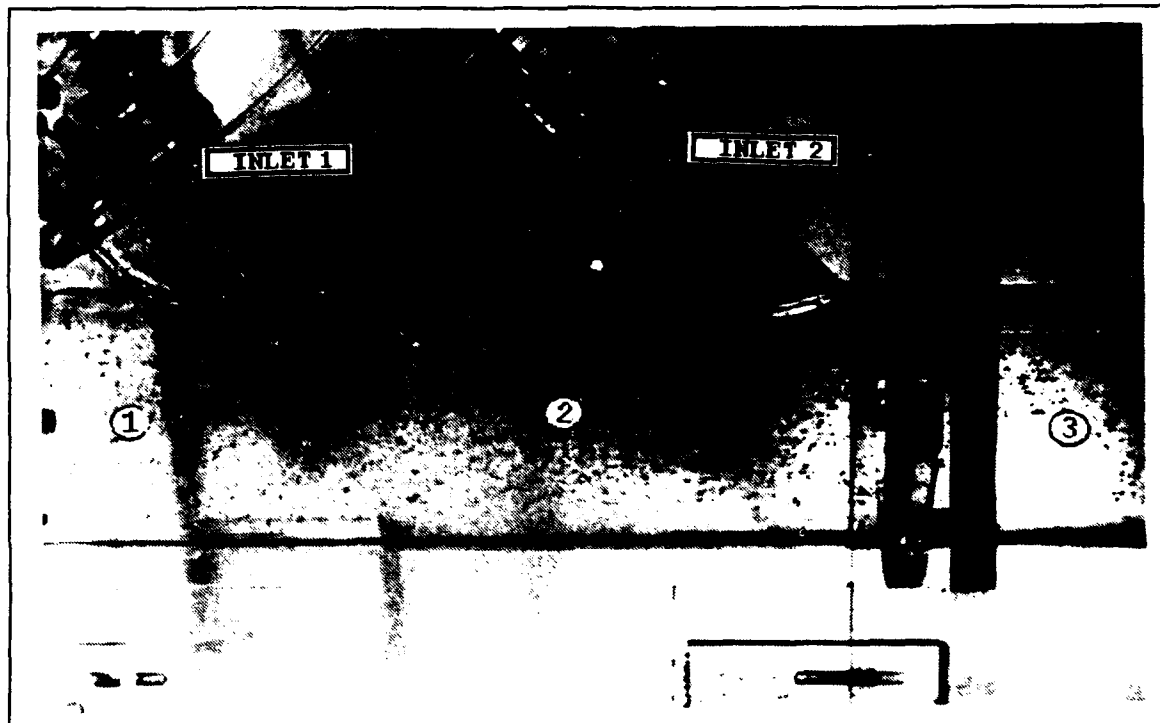


**Figure 3.18:** Configuration 3: Dual-Inlet, Axially-In-Line, Side-Dump Combustor

inlets made this flow field unique in comparison to the other configurations.

*a. The Dome Region*

The flame-holding or dome region had the same structural characteristics as the single-side-dump combustor. The region had a centrally-located, longitudinal circulation pattern, a clockwise rotation of fluid around the centerline near the dome, and two counter-rotating vortices leaving the region. The dome-region longitudinal structure is shown by Figure 3.19.

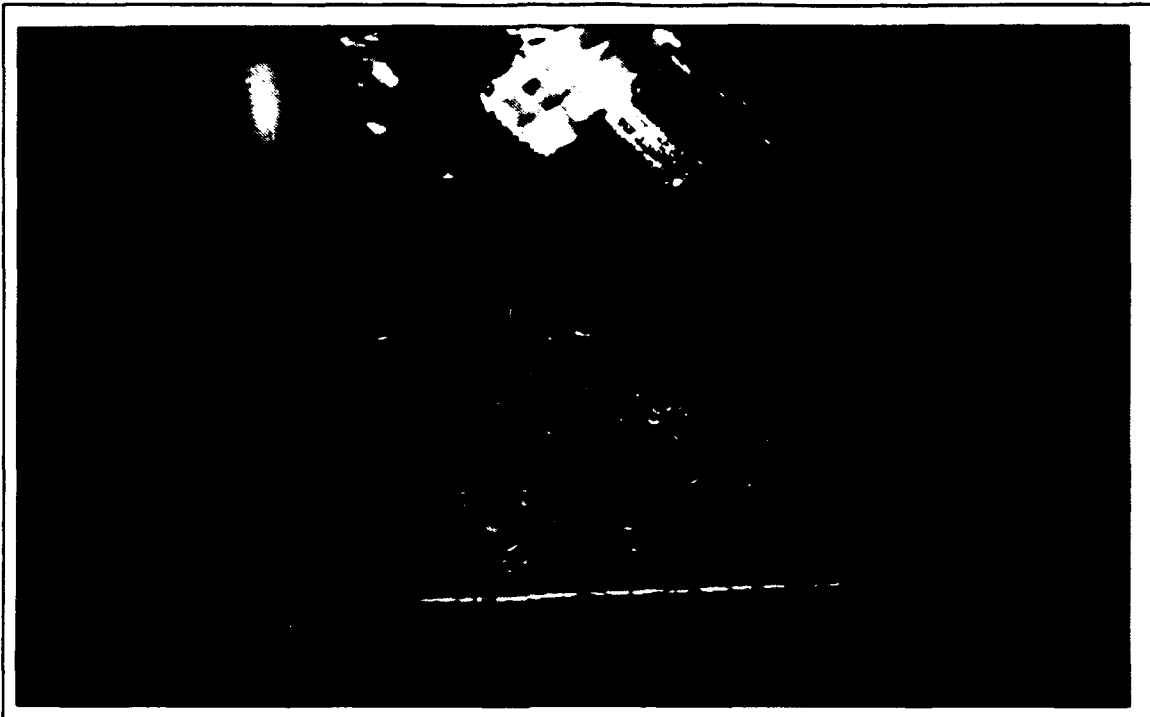


**Figure 3.19:** Configuration 3; Dome Region,  $L_d = -3"$ ,  $L_{lx} = 0"$

**b. Inlet-Jet Expansion and Impingement Regions**

Two inlet side dumps delivered fluid to this combustor configuration. Fluid from the first inlet (most upstream inlet) was divided between the flame-holding region, the ancillary-combustion region and the main-combustion region. Figure 3.20 shows the region between inlet 1 and 2. Fluid moving into the ancillary-combustion region was primarily the result of the inlet streamtube impinging on the curved lower combustor wall and following the wall circumferentially up into the region between the inlets [Figure 3.21]. Also, some fluid from the inlet streamtube moved into this region at the combustion chamber top as a result of the vortices formed between the high and low

velocity flows. Figure 3.20 also shows that there was only a weak circulation in the longitudinal direction in region 2.

As shown in Figure 3.22, no fluid flow from the second inlet was able to move upstream to form a recirculating region. Fluid from the second inlet jet primarily moved downstream into the main combustion region. This was attributed to the structure in the upstream regions and the mass flow from the first inlet.

### c. The Mixing or Ancillary Combustion Region

Figures 3.23 and 3.24 show the structure of the ancillary-combustion region (region 2). This region was confined by the two inlet jets. The region occupied the top

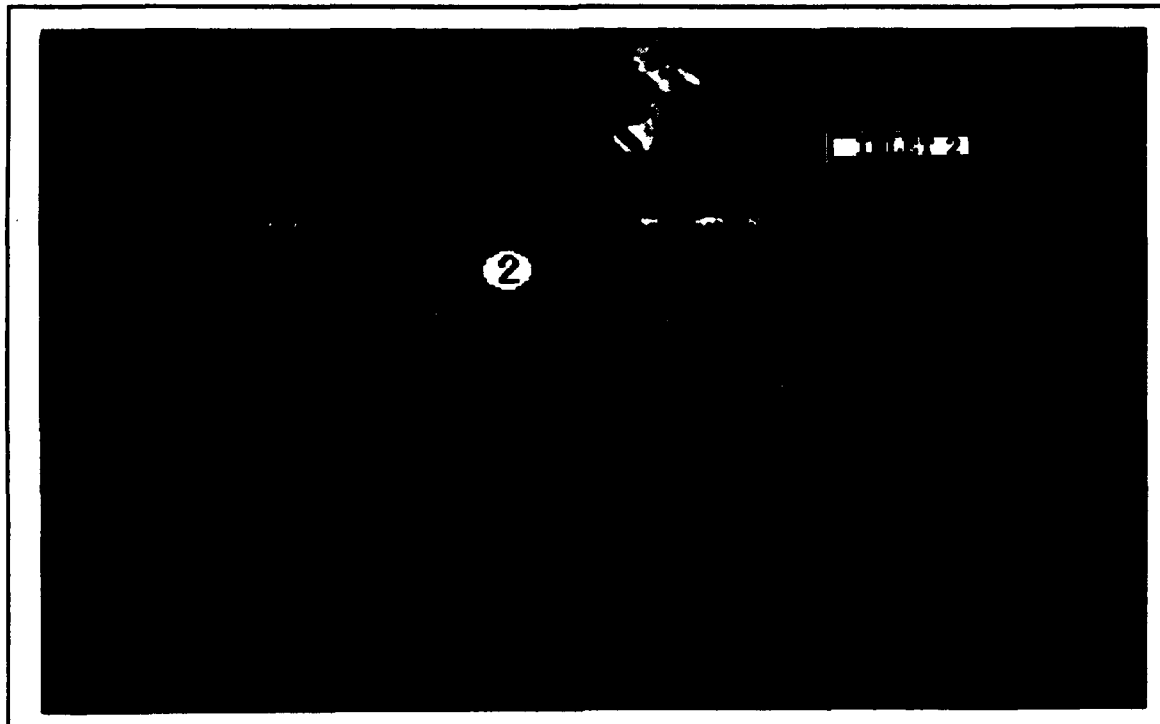
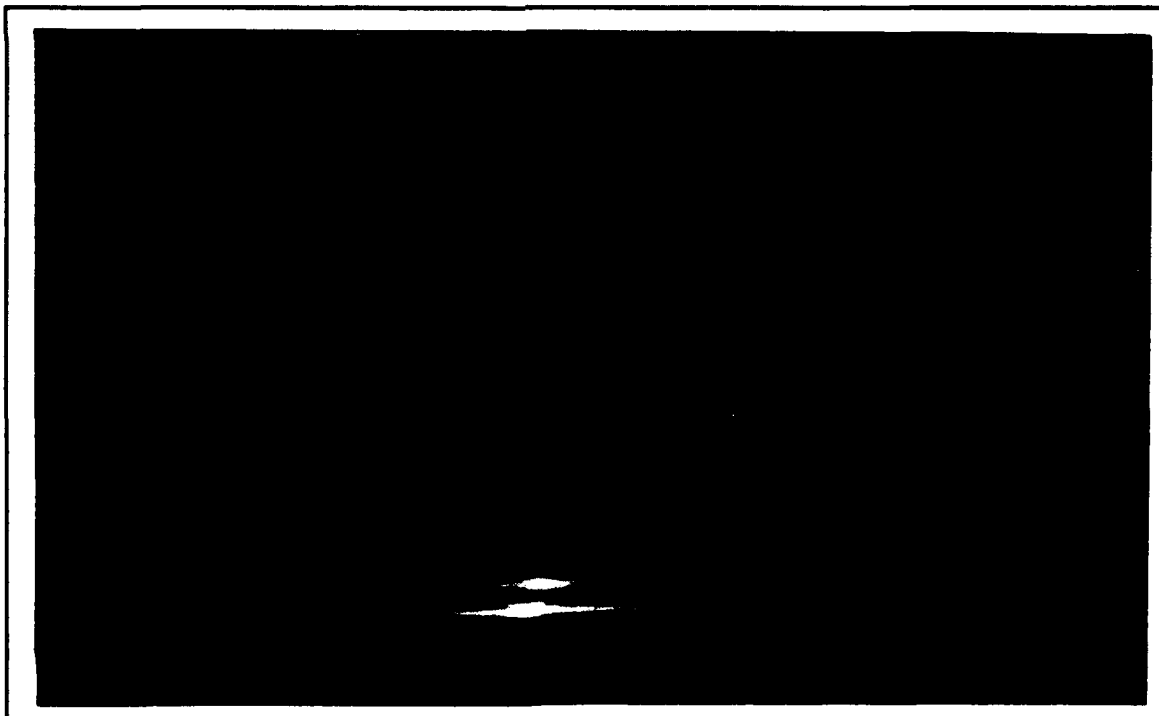


Figure 3.20: Configuration 3; Region 2,  $L_d = -3"$ ,  $L_{1x} = 0"$

portion of the combustion chamber and extended from approximately 0.77 D to 2.6 D along the longitudinal axis. Fluid entered the ancillary-combustion region primarily from the first inlet jet and from the counter-rotating vortices departing the dome region. As the inlet streamtube impinged the lower combustor wall the fluid flowed circumferentially around the side of the combustion chamber and combined with the side vortices, then moved into the ancillary-combustion region. The counter-rotating side vortices exhibited the twisting motion seen in Configuration 1. Only a small amount of fluid from the first inlet entered directly into region 2



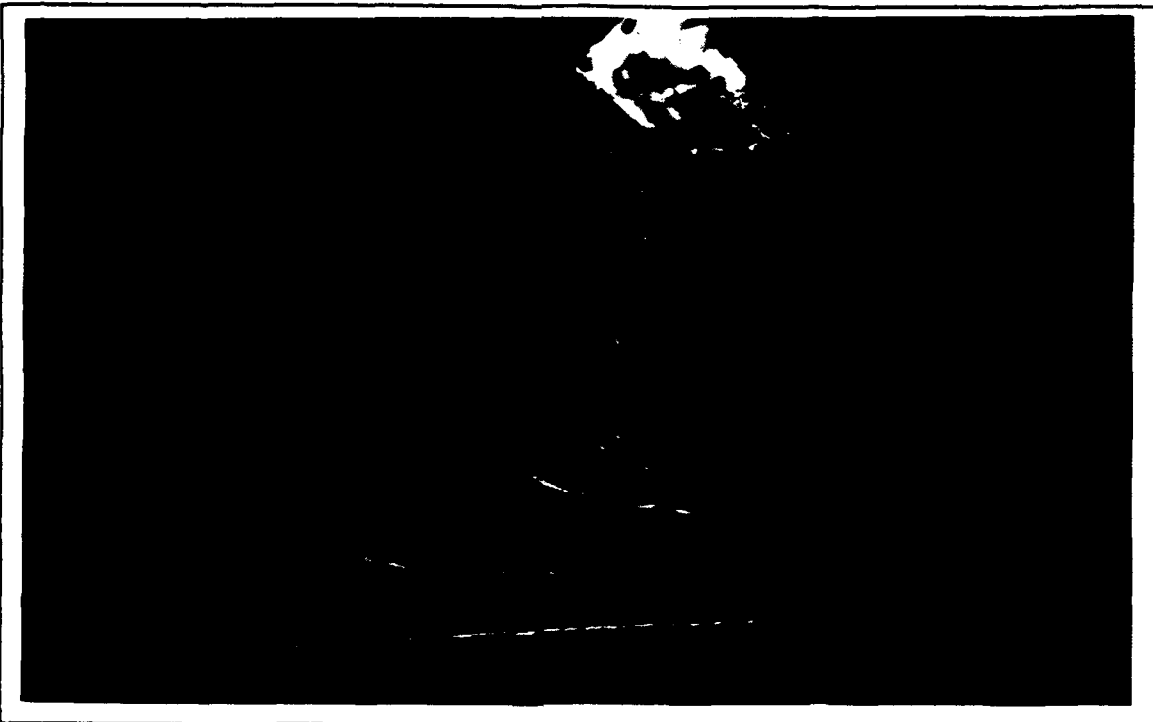
**Figure 3.21:** Configuration 3; Region 2,  $m_1/m_2=85/15\%$ ,  $L_d=-2"$ ,  $L_{1x}=1.5"$



Figure 3.22: Configuration 3;  $L_d = -2"$



Figure 3.23: Configuration 3;  $L_d = -4.5"$



**Figure 3.24:** Configuration 3; Region 2,  $m_1/m_2=85/15\%$ ,  $L_d=-4"$ ,  $L_{1x}=0"$

along the top of the combustor wall. These flow dynamics in a second recirculation zone could potentially provide increased wider flammability limits and combustion efficiency.

#### *d. The Main Combustion Region*

The main combustion region (region 3) exhibited the same twisting of streamtubes that was observed in the other configurations. The flow expanded, fully occupying the combustion chamber at 4 D from the longitudinal zero reference point. This was only 2.1 D from the upstream edge of the second inlet interface with the combustion chamber. However,

the total distance required to obtain good mixing increased in comparison with configuration 1 due to the second inlet. This difference between Configurations 1 and 3 is attributed to the reduced mass flow conditions and the effect of the ancillary combustion region on the swirl and twist of the side vortices.

## **2. Impact of Dome Length ( $L_d/D$ ) on Flow Stability and Mixing in the Dome and Main Combustion Regions**

### **a. The Dome Region**

The optimum dome lengths for flame stabilization and fluid mixing in the dome region were found to be between 0.62 and 1.4 D, except for  $m_1/m_2=100/0\%$ . In the latter case it was 0.54 D to 1.2 D, similar to the results for Configuration 1 (Figure 3.25). In these regions, the flow field was stable with no vortex shedding evident, and the fluid was steadily and uniformly mixed. For a mass flow rate ratio of 85/15%, no steady vortex pattern was formed in the center of the dome region until a dome length of 1.4 D. This dome length was 1.5 D for all other mass flow ratios. For dome lengths shorter than 0.54 D, the flow field was very unsteady with nearly periodic vortex shedding observed in the dome region.

### **b. The Main and Ancillary-Combustion Region**

No impact on the flow field stability was observed in region 2 or 3 due to changes in dome length or mass flow ratios, except for the ~~r~~test dome lengths where the entire

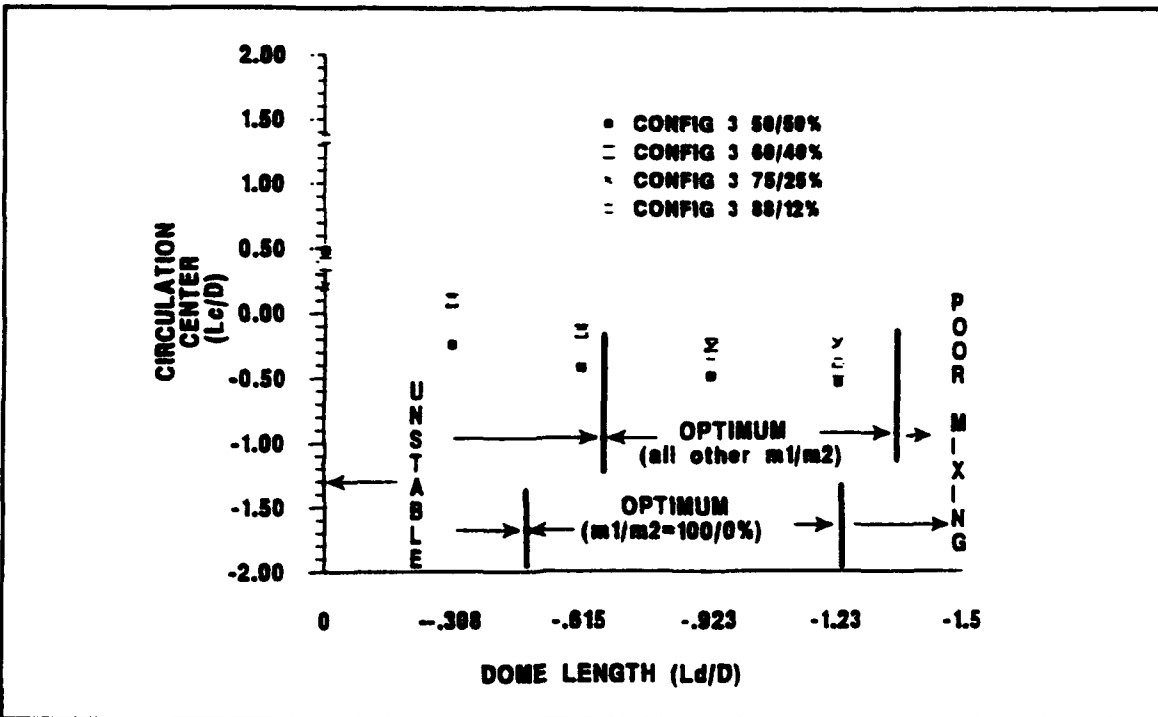


**Figure 3.25:** Configuration 3; Longitudinal Circulation Center ( $L_c$ ) Verses Dome Length ( $L_d$ )

combustor flow field surged to balance the oscillatory mass flow rates into the dome region.

### 3. Impact of Mass Flow Ratio

Five mass flow conditions between the inlets were investigated. The mass flow conditions were varied from 50/50% to 100/0% (upstream inlet/downstream inlet). As the mass flow in the forward inlet was increased, the structured flow field of the ancillary-combustion region shown in Figure 3.26 deteriorated to the flow field structure of Figure 3.27. Finally, at a mass flow condition of 100/0% the ancillary-combustion region did not exist, and the flow field

was essentially the same as observed for the single-side-dump configuration. A corresponding change in the main combustion region was observed, with the mixing quality of the region increasing as the upstream inlet mass flow increased. No impact on the dome region was observed for changes in mass flow condition. Thus, higher upstream flow rates hindered the beneficial effects of the second recirculation region (region 2), but enhanced the mixing downstream. Variable air flow distributions may thus be able to provide the optimum combination of flammability and combustion efficiency for varying flight conditions.

**4. "Fuel" Injection Pattern Impact on "Fuel" Distribution**

**a. Impact of "Fuel" Injector Location on "Fuel" Distribution in the Dome Region**

As shown by Figure 3.28, the lower area of the inlet region in the forward inlet provides the "fuel" into the dome region. This is in agreement with the results from Configuration 1 and 2. Some "fuel" injected at other locations within the inlet duct can enter the dome region, but only in small quantities, and in an unsteady manner.

**b. Impact of "Fuel" Injector Location on "Fuel" Distribution in the Ancillary Combustion Region**

Figure 3.28 also shows that most of the "fuel" that enters the ancillary combustion region comes from injection

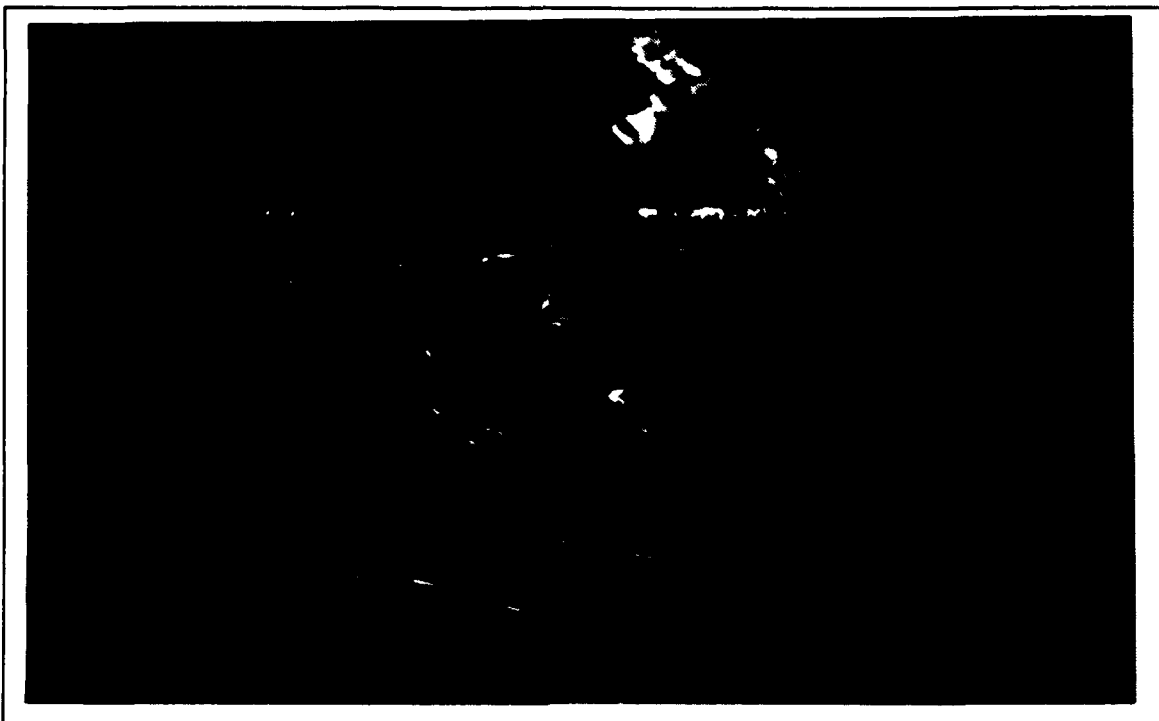


**Figure 3.26:** Configuration 3; Region 2,  $m_1/m_2=50/50\%$ ,  $L_d=-2"$ ,  
 $L_{1x}=0"$

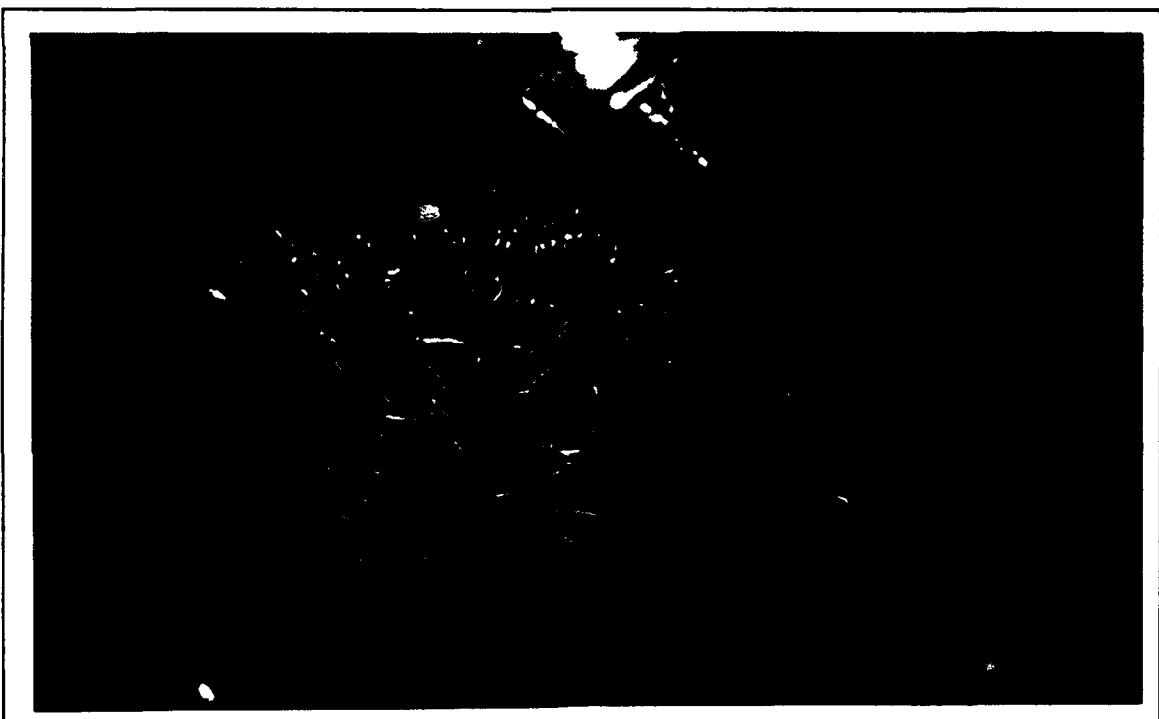


**Figure 3.27:** Configuration 3; Region 2,  $m_1/m_2=85/15\%$ ,  $L_d=-2"$ ,  
 $L_{1x}=0"$

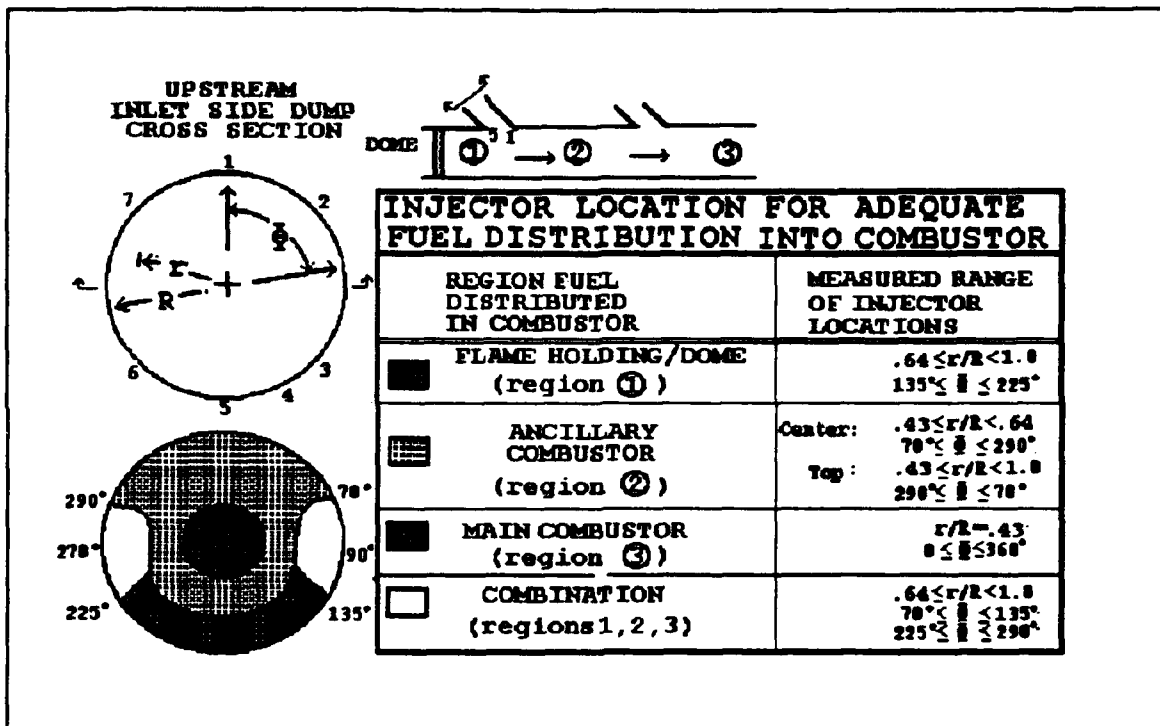


**Figure 3.28:** Impact of "Fuel" Injection Location on "Fuel" Distribution, Configuration 3

locations near the downstream side of the first inlet, and from an annular area surrounding the center of the inlet. "Fuel" injection on the right and left sides of the inlet was also distributed into this region, but the rate was smaller and unsteady. "Fuel" injection from locations in the downstream inlet did not penetrate upstream (see Figure 3.23).

**c. Impact of "Fuel" Injector Location on "Fuel" Distribution in the Main Combustion Region**

The major part of the "fuel" in the main combustion region came from the center of the upstream inlet and all locations within the downstream inlet. "Fuel" injection in the center of the upstream inlet moved into the combustion

chamber, along the bottom wall of the chamber, and then into the main combustion region. However, in order to have "fuel" uniformly distributed in the combustion region, it also had to be injected into the downstream inlet.

**D. COMPARISON OF THE RESULTS WITH OTHER INVESTIGATIONS**

Table 3.1 shows a summary of results from this investigation compared with the available data in the open literature. Overall, there was good agreement between the results of this study, and previous studies, when minor differences in geometric configuration are considered.

**Table 3.1: SUMMARY AND COMPARISON OF RESULTS FOR SIDE DUMP COMBUSTORS**

GEOMETRIC CONFIGURATION	DOME LENGTH (L <sub>d</sub> /D)	OPTIMUM LOCATION FOR "FUEL" INJECTION IN INLET SIDE DUMP		
		Current Optimal	Other Results	Flame Holding Region Main Combustor
Single Side Dump $\theta=45^\circ$ ; $A_3/A_2=1.69$	-1.1 to -0.5	- 1 <sup>1</sup> -1.5 <sup>2,3</sup>		0.7sr/Rs1.0 135° ≤ θ ≤ 225°  Center: 0sr/Rs1.7 0° ≤ θ ≤ 360° Top: 0sr/Rs1 290° ≤ θ ≤ 70°
Dual Side Dump $\theta=45^\circ$ ; 90° Opposed; $A_3/A_2=1.72$	-0.68 to -0.31	- - 1 <sup>4</sup> 0 to -1 <sup>5</sup>		.64sr/Rs1.0 135° ≤ θ ≤ 225°  .64sr/Rs1 135° ≤ θ ≤ 70° 290° ≤ θ ≤ 225°  0sr/Rs1.0 290° ≤ θ ≤ 70°
Dual In-Line Side Dump $\theta=45^\circ$ ; $A_3/A_2=1.72$	$m_1/m_2$  100%: -1.2 to -.54  others: -1.4 to -.62	none		Region 1, inlet1: .64sr/Rs1 135° ≤ θ ≤ 225°  Region 2, inlet1: .43sr/Rs.64 70° ≤ θ ≤ 290°  .43sr/Rs1 290° ≤ θ ≤ 70°  Region 3: inlet1: r/R=.43 0° ≤ θ ≤ 360° inlet2: all

Notes:

- 1 Petkus and Jaul, [Ref. 6]; single side dump;  $\theta=90^\circ$
- 2 Onn, S.-C et. al., [Ref. 5]; single side dump; Ducted Rocket;  $\theta=45^\circ$
- 3 Choudhury, [Ref. 9]; Swirler with multiple side dumps,  $\theta=45^\circ$
- 4 Liou and Wu, [Ref. 7]; dual side dumps,  $\theta=60^\circ, 180^\circ$  radially opposed
- 5 Stull et. al., [Ref. 8]; dual side dumps,  $\theta=45^\circ, 90^\circ$  radially opposed
- 6 Zetterström and Sjöblom, [Ref. 10];  $\theta=45^\circ, 150^\circ$  radially opposed

#### IV. CONCLUSIONS

Three different configurations for an inlet-side-dump, ramjet combustor were investigated in model tests. Non-intrusive laser-sheet, water-tunnel, flow-visualization techniques were successfully utilized to qualitatively evaluate and determine optimum flame-stabilization dome lengths and fuel-injection locations. The results obtained for the single-side-dump combustor and the dual side dump, 90° separated, combustor were in good agreement with the results from previous studies with similar geometric configurations. The following major conclusions were made from the present results:

1. The (optimum) dome lengths which provided good "fuel" distribution and steady mixing were between 0.31 D and 1.4 D in all cases. Shorter dome lengths generally resulted in unstable flow in the dome region, and longer dome lengths resulted in poor mixing.
2. For all three configurations, fuel injection in a narrow region on the upstream side of the inlet cross section was the only location capable of distributing "fuel" into the flame holding region.
3. Multiple injection locations in the inlet cross section are required to distribute "fuel" uniformly into the downstream main combustion region.

4. Dome length had no impact on the mixing quality in the main combustion regions of all three configurations, except for very short dome lengths, which induced oscillatory flow.

5. Of the three combustor configurations, the dual, axially-in-line side-dump configuration demonstrated the best potential for increasing performance across a wide range of operating conditions. This is attributable to the ancillary combustion region between the inlets, and to the ability to control the size and strength of the region by varying air mass flow through the two inlet dumps.

Additional work is required to characterize the combustor performance under reacting flow conditions. A parametric test series is needed to determine if the optimum configurations from this flow visualization study will result in the optimum combustion efficiency and/or flammability limits.

#### LIST OF REFERENCES

1. Curran, E.T., Lerngang, J.L., and Donaldson, W. A., "Review of High Speed Air Breathing Propulsion Systems," Proceedings of the Eighth International Symposium on Air Breathing Engines, AIAA, Washington D.C., June 1987.
2. Zarlingo F.C., "Overview of Propulsion Concepts for Tactical Missiles," AGARD-CP-493.
3. Mongia, H. C., "Application of CFD in Combustor Design Technology," Journal of Propulsion and Power, Vol.4, January - February 1989, pp. 48-53.
4. Milshtein,T. and Netzer, D.W., "Three-Dimensional, Primitive-Variable Model for Solid-Fuel Ramjet Combustion," Journal of Spacecraft and Rockets, Vol. 23, January-February 1986,p.113.
5. Onn S.-C., Chiang H.-J., Hwang, H.-C, and Wei, J.-K., "Optimization of Operation Conditions and Configurations for Solid-Propellant Ducted Rocket Combustors," AIAA/SAE/ASME/ASEE 29th Joint Propulsion Conference, Monterey, California, 28-30 June 1993.
6. Petkus, E.P.,and Jaul, W.K., "Investigation of the Flow Field in a Side Dump Combustor Under Cold flow Conditions Using LDV Techniques," 18th JANNAF Combustion Meeting, Pasadena, California, 19-23 October 1981.
7. Liou, T.-M. and Wu, S.-M., "The Flowfield in a Dual Inlet Side Dump Combustor," Journal of Propulsion and Power, Vol.4, January - February 1988, pp.52-60.
8. Stull, F.D., Craig, R.R., Streby, G.D.,and Vanka, S.P., "Investigation of a Dual Inlet Side Dump Combustor Using Liquid Fuel Injection," Journal of Propulsion and Power, Vol. 1, January - February 1985, pp. 83-88.
9. Choudhury, P.R., "Characteristics of A Side Dump Gas Generator Ramjet," AIAA/SAE/ASME 18th Joint Propulsion Conference, Cleveland, Ohio, June 1982.
10. Zetterström, K-A.,and Sjöblom, B., "An Experimental Study of Side Dump Ramjet Combustors," ISABE paper number 85-7024.

11. Naval Weapons Center Technical Publication 6209, *Static and Dynamic Performance Investigation of Side Dump Ramjet Combustors: Test Summary* by W.H. Clark, December 1980.
12. Eidetics International Inc., *Flow Visualization Water Tunnel: Operators Manual*, 1990
13. Merzkirch, W., *Flow Visualization*, 2nd Edition, pp. 14-48, Academic Press Inc., 1987.
14. Schadow, K.C., "Boron Combustion in Ducted Rockets," *Ramjets and Ramrockets for Military Applications*, AGARD-CP-307, October 1981.
15. Merzirch, W., "Techniques of Flow Visualization," AGARD-AG-302, December 1987.
16. Shahaf, M., Goldman, K., and Greenberg, J.B., "An Investigation of Impinging Jets in Flow with Sudden Expansion," Israel Journal of Technology, Vol. 18, 1980, pp. 57-64.

### INITIAL DISTRIBUTION LIST

- |    |  |   |
|----|--|---|
| 1. | Defense Technical Information Center<br>Cameron Station<br>Alexandria, Virginia 22304-6145   | 2 |
| 2. | Naval Air Warfare Center<br>Weapons Division, Code 32463<br>China Lake, California 93555-6001  | 1 |
| 3. | Library, Code 52<br>Naval Postgraduate School<br>Monterey, California 93943-5000   | 2 |
| 4. | Department Chairman, Code AA<br>Department of Aeronautics and Astronautics<br>Naval Postgraduate School<br>Monterey, California 93943-5000             | 1 |
| 5. | Professor David W. Netzer, Code AA/Nt<br>Department of Aeronautics and Astronautics<br>Naval Postgraduate School<br>Monterey, California 93943-5000    | 2 |
| 6. | Professor Raymond P. Shreeve, Code AA/Se<br>Department of Aeronautics and Astronautics<br>Naval Postgraduate School<br>Monterey, California 93943-5000 | 1 |
| 7. | Major Ronald F. Salyer<br>1818 E. Meadowview Drive<br>Statesville, North Carolina 28677-5000   | 2 |